

ARTICLE TYPE**Gaia Search for stellar Companions of TESS Objects of Interest IV**

M. Mugrauer | J. Rück | K.-U. Michel

Astrophysikalisches Institut und
Universitäts-Sternwarte Jena**Correspondence**M. Mugrauer, Astrophysikalisches Institut
und Universitäts-Sternwarte Jena,
Schillergäßchen 2, D-07745 Jena, Germany.
Email: markus@astro.uni-jena.de

arXiv:2306.02452v1 [astro-ph.SR] 4 Jun 2023

We present the latest results of our ongoing multiplicity study of (Community) TESS Objects of Interest, using astrometric and photometric data from the ESA-Gaia mission to detect stellar companions of these stars and characterize their properties. A total of 134 binary, 6 hierarchical triple, and two quadruple star systems are identified among 1106 targets whose multiplicity is investigated in the course of our survey, located at distances closer than about 500 pc around the Sun. The detected companions and targets are at the same distance and have a common proper motion, as expected for components of gravitationally bound stellar systems, as demonstrated by their accurate Gaia DR3 astrometry. The companions have masses from about 0.11 to $2 M_{\odot}$ and are most abundant in the mass range between 0.2 and $0.5 M_{\odot}$. The companions have projected separations from the targets between about 50 and 9700 au. Their frequency is the highest and constant from about 300 up to 750 au, decreasing at larger projected separations. In addition to main sequence stars, four white dwarf companions are detected in this study, whose true nature is revealed by their photometric properties.

KEYWORDS:

binaries: visual, white dwarfs,

stars: individual (TOI 3714 B, TOI 3984 B, TOI 4301 B, CTOI 13073396 B)

1 | INTRODUCTION

In 2020 we initiated a new survey at the Astrophysical Institute and University Observatory Jena with the aim to explore the multiplicity of (Community) TESS Objects of Interest ((C)TOIs), i.e. stars photometrically monitored by the Transiting Exoplanet Survey Satellite (TESS, Ricker et al., 2015), which show promising dips in their light curves, possibly caused by exoplanets orbiting these stars.

In our survey, stellar companions of (C)TOIs are detected and their properties are determined with astrometry and photometry, originally from the 2nd data release (Gaia DR2 from hereon, Gaia Collaboration et al., 2018) and later from the early version of the 3rd data release (Gaia EDR3 from hereon, Gaia Collaboration et al., 2021) of the ESA-Gaia mission. The first results of the survey were presented by Mugrauer and Michel

(2020), Mugrauer and Michel (2021), and Mugrauer, Zander, and Michel (2022), who have already examined the multiplicity of more than 4100 (C)TOIs, all of which are listed in the (C)TOI release of the Exoplanet Follow-up Observing Program for TESS (ExoFOP-TESS)¹. Meanwhile, several of these (C)TOIs discovered as members of multiple star systems in the course of our survey have already been confirmed as exoplanet host stars by follow-up observations, e.g. TOI 179, TOI 277, TOI 954, TOI 1228, TOI 1246, TOI 1410, TOI 1452, TOI 1516, TOI 1690, TOI 1710, TOI 1749, TOI 1797, TOI 1801, TOI 2152, TOI 2193, and TOI 2459, which are listed in the Extrasolar Planets Encyclopaedia (see Schneider, Dedieu, Le Sidaner, Savalle, & Zolotukhin, 2011, and references therein)².

¹Online available at:https://exofop.ipac.caltech.edu/tess/view_toi.phphttps://exofop.ipac.caltech.edu/tess/view_ctoi.php²Online available at: <http://exoplanet.eu/>

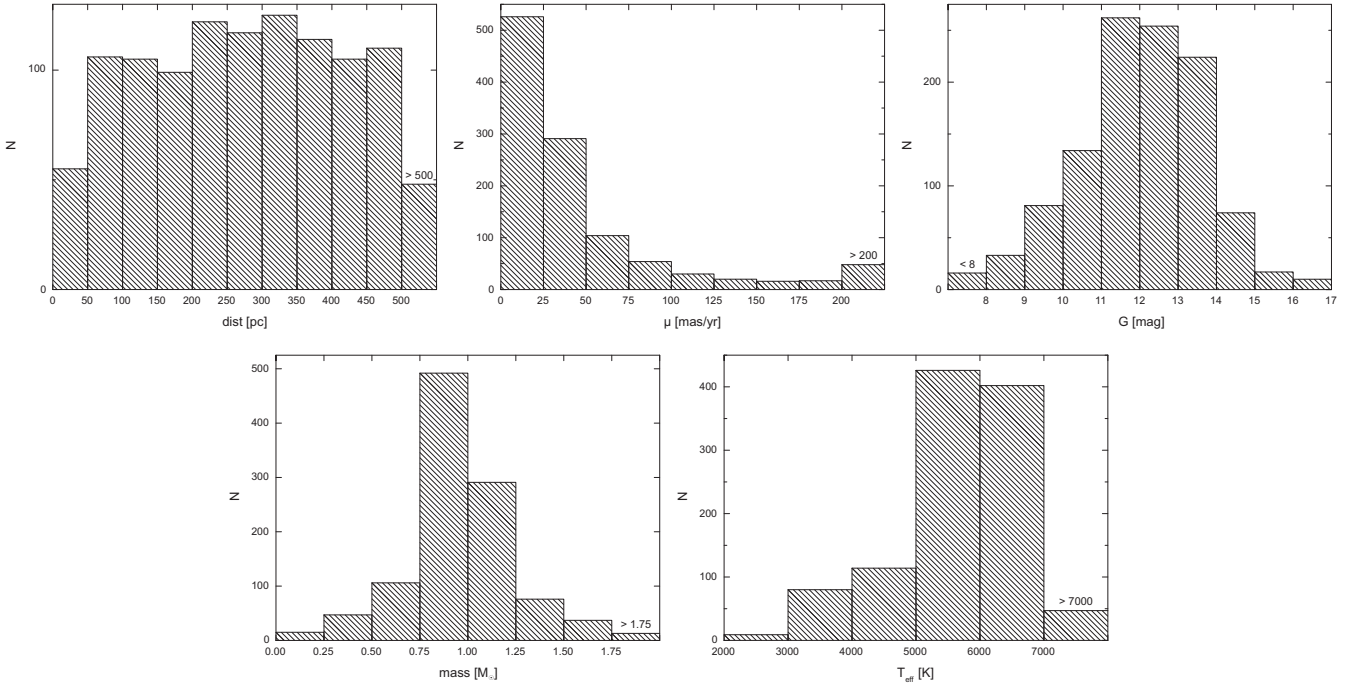


FIGURE 1 The histograms of the individual properties of the targets in this study. The histograms of distance ($dist$), total proper motion (μ), and G-band magnitude are based on the Gaia DR3 data of all 1106 targets. Masses and effective temperatures (T_{eff}) have been taken from the Starhorse catalog where available, which is the case for 1078 targets.

Thanks to the successful execution of the TESS mission and the photometric analysis of its data, the number of (C)TOIs, and thus the number of targets for our survey, is continuously growing. In this paper, we search for companions of more than thousand (C)TOIs reported by the ExoFOP-TESS, whose multiplicity has not yet been studied in our survey, using the latest data release from the ESA-Gaia mission.

In the following section we describe in detail the properties of the selected targets and the search for companions around these stars. In Section 3 we present all (C)TOIs with detected companions and characterize the properties of these stellar systems. Finally, we summarize the current status of our survey and give an outlook on the project in the last section of this paper.

2 | SEARCH FOR STELLAR COMPANIONS OF (C)TOIS BY EXPLORING THE GAIA DR3

The companion search presented here uses astrometric and photometric data from the 3rd data release of the ESA-Gaia mission (Gaia DR3 from hereon, Gaia Collaboration et al., 2022), obtained with the instruments of the ESA-Gaia satellite during the first 34 months of its mission. This data release contains astrometric solutions, i.e. position (α , δ), parallax π ,

and proper motion ($\mu_\alpha \cos(\delta)$, μ_δ) of about 1.5 billion sources down to a limiting magnitude of 21 mag in the G-band, which means white light observations exploiting the entire spectral sensitivity range of the used CCD detectors.

Parallaxes are measured with an uncertainty in the range of about 0.02 milliarcsec (mas) for bright ($G < 15$ mag, with a lower limit of $G \sim 1.7$ mag) up to 0.5 mas for faint ($G = 20$ mag) detected sources. Proper motions are determined with an accuracy of about 0.02 mas/yr for bright objects, deteriorating to 0.6 mas/yr for $G = 20$ mag. In addition, the G-band magnitude of all sources is recorded with a photometric uncertainty ranging from about 0.3 millimagnitude (mmag) for the brightest to 6 mmag for faint sources.

In the study presented here, stellar companions of the investigated (C)TOIs are firstly identified as sources that are at the same distance as the targets and secondly have a common proper motion with these stars. In order to unambiguously detect co-moving companions and confirm their equidistance to the (C)TOIs, we consider in our study only those sources listed in the Gaia DR3 for which there is a significant measurement of parallax ($\pi/\sigma(\pi) > 3$) and proper motion ($\mu/\sigma(\mu) > 3$). Sources with a negative parallax are ignored.

Since our survey was originally based on Gaia DR2 data, with a typical parallax uncertainty of 0.7 mas for faint sources

down to $G = 20$ mag, it is restricted to (C)TOIs within 500 pc of the Sun (i.e. $\pi > 2$ mas), to ensure that $\pi/\sigma(\pi) > 3$ also applies to the faintest detectable companions. This distance constraint is slightly relaxed to $\pi + 3\sigma(\pi) > 2$ mas, i.e. the parallax uncertainty of the (C)TOIs is also taken into account. Although we are now using Gaia DR3 data, which exhibit a smaller parallax uncertainty, we retain the chosen distance constraint for the survey for continuity.

In this paper, we explore the multiplicity of 1106 targets³ that have not yet been investigated in the course of our survey with Gaia DR3 data, that meet the distance constraint described above and are therefore selected as targets for the study presented here. Figure 1 illustrates the properties of the selected targets with histograms. The distance ($dist$) and total proper motion (μ) of all targets are determined using their precise Gaia DR3 parallax ($dist[\text{pc}] = 1000/\pi[\text{mas}]$) and proper motion in right ascension and declination. The G-band magnitude of all targets is listed in the Gaia DR3, while their mass and effective temperature (T_{eff}) are taken from the Starhorse catalog (SHC from here on, Anders et al., 2019) where available, which is the case for 1078 stars, i.e. the vast majority ($\sim 97\%$) of all 1106 targets. The targets have distances from the Sun between about 6 to 840 pc.

The distance distribution of the target sample examined here is rather flat compared to the distribution of the distance of the targets investigated earlier in this survey, which shows a peak at about 100 pc. This difference in distance distribution results from the unequal distance distributions of the TOIs and CTOIs in the target sample studied here. While the CTOIs have a peak in their distance distribution at about 100 pc, similar to the targets whose multiplicity was examined earlier in this survey, the TOIs are located at greater distances from the Sun and are most frequently found at about 350 pc. Due to their smaller distance, the CTOIs also appear brighter (by about 1 mag on median) and have proper motions that are on median about 1.5 times higher than those of the TOIs.

The targets studied here have proper motions in the range between about 1 and 1660 mas/yr⁴, G-band magnitudes from 3.4 to 17 mag⁵ masses between about 0.14 and $3.8 M_{\odot}$, and effective temperatures ranging from about 2700 up to 10100 K. Based on the cumulative distribution functions of the individual properties, the targets are most commonly located at

distances between about 50 and 500 pc have typical proper motions from about 5 to 30 mas/yr, and G-band magnitudes from about $G = 11$ to 14 mag. The targets are mainly solar-like stars with masses in the range between about 0.7 and $1.3 M_{\odot}$. This population is also evident in the T_{eff} -distribution of the targets at intermediate temperatures around 4500 to 6500 K. An additional but weaker clustering of targets is found in this distribution at lower effective temperatures between about 3400 and 4400 K, namely the early M to mid K dwarf population.

As defined and described in Mugrauer and Michel (2020), our survey is restricted to companions with projected separations up to 10000 au, which on the one hand guarantees an effective companion search, but on the other hand also detects the vast majority of all wide companions of the selected targets. This results in an angular search radius for companions around the targets of $r[\text{arcsec}] = 10\pi[\text{mas}]$, with π the Gaia DR3 parallax of the (C)TOIs.

All sources listed in Gaia DR3 that are located within the search radius used around the targets and have a significant parallax and proper motion are considered companion-candidates. A total of about 33000 such objects are detected around 891 targets, whose multiplicity is investigated in this study. The companionship of all these candidates is tested using their precise Gaia DR3 astrometry and that of the associated (C)TOIs, following exactly the procedure described in Mugrauer and Michel (2020). The vast majority of these sources can be excluded as companions because they do not have a common proper motion with the (C)TOIs and/or are not at the same distance as these stars. In contrast, 149 candidates can be unambiguously confirmed as companions of the (C)TOIs with their accurate Gaia DR3 astrometry. The properties of these companions and the associated (C)TOIs are described in detail in the next section of this paper.

3 | (C)TOIS AND THEIR DETECTED STELLAR COMPANIONS

The mass, effective temperature and absolute G-band magnitude of most of the (C)TOIs with detected companions presented here are listed in the SHC, and we show these stars in a $T_{\text{eff}}-M_G$ -diagram in Figure 2. In this diagram we plot the main sequence of Pecaut and Mamajek (2013)⁶ for comparison.

Most targets with detected companions are main sequence stars. Only a few (C)TOIs are (significantly) located above the main sequence, and these stars also have surface gravities of $\log(g[\text{cm/s}^2]) < 3.8$, as listed in the SHC, and are therefore classified as (sub)giants.

³The target sample consists of 747 TOIs and 359 CTOIs, i.e. approximately twice as many TOIs as CTOIs. The relative frequency of CTOIs among the targets examined here is about 1.3 times higher than the relative frequency of these objects among the targets whose multiplicity was previously examined in the course of this survey.

⁴The median of the proper motion of the targets studied here is 26 mas/yr which is just slightly lower than the median of the proper motion of the targets studied earlier in this survey ($Mdn(\mu) = 32$ mas/yr).

⁵The targets whose multiplicity is investigated here have a G-band magnitude of 12 mag on median which is one magnitude fainter than the median magnitude of the targets studied before in the course of this survey.

⁶Online available at: http://www.pas.rochester.edu/~emamajek/EEM_dwarf_UBVIJHK_colors_Teff.txt. Version 2022.04.16 is used here.

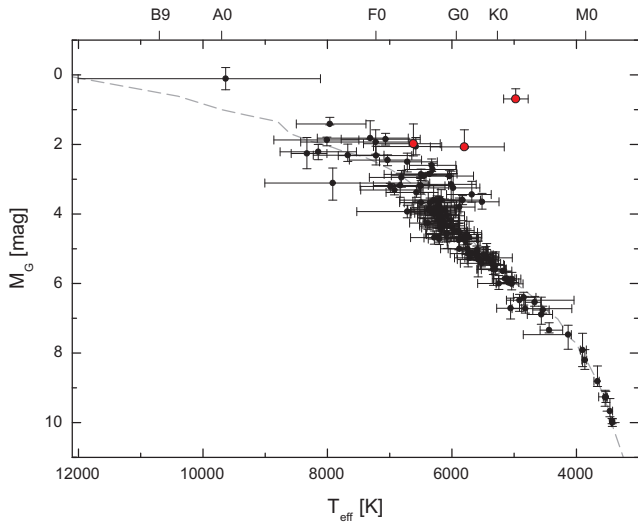


FIGURE 2 The $T_{\text{eff}}-M_G$ -diagram of (C)TOIs with detected companions presented here. (C)TOIs listed in the SHC with surface gravities $\log(g[\text{cm/s}^{-2}]) < 3.8$ are shown as red circles, those with larger surface gravities with black circles, respectively. The main sequence is plotted as a grey dashed line.

The parallax, proper motion, apparent G-band magnitude, and extinction estimate of the (C)TOIs and their companions detected in this study are summarized in Table 3, which lists a total of 134 binary, 6 hierarchical triple, and two quadruple star systems.

We determine the angular separation (ρ) and the position angle (PA) of all detected companions to the associated (C)TOIs, using the precise Gaia DR3 astrometry of each object. The derived relative astrometry of the companions is listed in Table 4, together with its uncertainty, which remains below about 1.3 mas in angular separation or 0.08° in position angle.

Table 4 also summarizes the parallax difference $\Delta\pi$ between the (C)TOIs and their companions, together with its significance $\text{sig-}\Delta\pi$, which is also calculated taking into account the astrometric excess noise of each object. The same table lists for each companion its differential proper motion μ_{rel} relative to the associated (C)TOI with its significance, and its cpm-index ⁷.

The parallaxes of the individual components of the stellar systems presented here are not significantly different from each other ($\text{sig-}\Delta\pi < 3$) when the astrometric excess noise is taken into account. This clearly proves the equidistance of the

detected companions with the (C)TOIs, as expected for components of physically associated stellar systems. All but one of the detected companions have a $\text{cpm-index} \geq 5$ and more than 95 % of them even have a $\text{cpm-index} \geq 10$, i.e. the detected companions and the associated (C)TOIs clearly form common proper motion pairs, as expected for gravitationally bound stellar systems. Note that for systems with small cpm-index and parallax, the possibility of random pairing is increased.

As we use astrometric data from the latest Gaia data release in this study, it is worth noting that the equidistance and common proper motion of all but two of the companions previously detected in this survey using Gaia DR2 astrometry (see Mugrauer & Michel, 2020), are confirmed by Gaia DR3 astrometry. While the cpm-index of almost all companions remains constant, the parallax difference between the detected companions and the (C)TOIs is reduced to about half with the more accurate Gaia DR3 astrometry, reinforcing the conclusion that these co-moving companions and the (C)TOIs are components of physically associated stellar systems. For TOI 737 B and TOI 851 B, their companionship could not be tested with Gaia DR3 astrometry because only their equatorial coordinates, but not their proper motion or parallax, are listed in the latest Gaia data release. However, according to their Gaia DR2 astrometry, both companions have a high degree of common proper motion (cpm-index of 29 and 57, respectively), and their differential proper motion does not significantly exceed the expected escape velocity. We therefore conclude that also these two stars are gravitationally bound companions of the associated TOIs.

The absolute G-band magnitudes of all detected companions are from the SHC or, if not available, from the SHC2 (Anders et al., 2022), indicated with the SHC2 flag in Table 5.

The SHC is based on several photometric catalogues as well as on Gaia DR2 astrometry and photometry, the SHC2 on the corresponding data of the Gaia EDR3. Where possible, we use the data from the SHC instead of the SHC2, since the properties of a larger number of detected companions but also (C)TOIs are listed in this catalogue than in the SHC2.

If the absolute magnitude of the companions is not listed in these catalogs, it is derived using the apparent G-band photometry of the companions as well as the parallax of the (C)TOIs, and the Apsis-Priam G-band extinction estimate listed in the Gaia DR2 if available, otherwise the G-band extinction from the SHC. The companion extinction estimate is used if available, otherwise that of the (C)TOIs.

The projected separation of all companions is determined from their angular separation from the associated (C)TOIs and the parallax of these stars.

The mass and effective temperature of the companions presented here, including their uncertainties, are from the SHC or the SHC2 (indicated by the SHC2 flag in Table 5) where

⁷The common proper motion (cpm) index, as defined in Mugrauer and Michel (2020), characterizes the degree of common proper motion of a detected companion with the associated (C)TOI.

TABLE 1 Photometry of three white dwarf companions detected in this study. For each companion we list the color difference $\Delta(B_p - R_p)$ and the G-band magnitude difference ΔG to the associated (C)TOI, its apparent $(B_p - R_p)$ color, as well as its derived intrinsic color $(B_p - R_p)_0$ and effective temperature T_{eff} .

Companion	ΔG [mag]	$\Delta(B_p - R_p)$ [mag]	$(B_p - R_p)$ [mag]	$(B_p - R_p)_0$ [mag]	T_{eff} [K]
TOI 3714 B	4.557 ± 0.004	-1.217 ± 0.078	1.100 ± 0.078	$0.859^{+0.110}_{-0.243}$	5632^{+809}_{-316}
TOI 3984 B	4.433 ± 0.005	-1.957 ± 0.099	0.557 ± 0.099	$0.440^{+0.128}_{-0.128}$	6999^{+615}_{-393}
CTOI 13073396 B	2.651 ± 0.004	-2.356 ± 0.011	0.138 ± 0.009	$-0.060^{+0.043}_{-0.035}$	10015^{+450}_{-512}

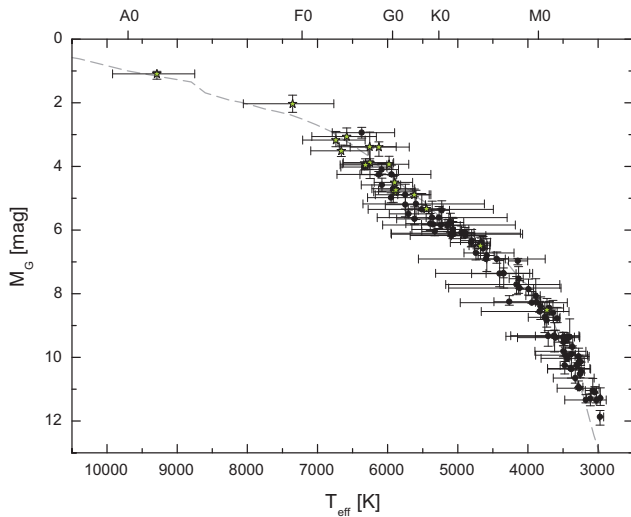


FIGURE 3 This $T_{\text{eff}}-M_G$ -diagram shows all detected companions whose effective temperatures are listed in either the SHC or SHC2, or for which Apsis-Priam temperature estimates are available. Companions, which are the primary components of their stellar systems, are shown as green star symbols. The main sequence is plotted as a dashed grey line for comparison.

available, which is the case for about 73 % of all companions. We plot these companions in Figure 3 in a $T_{\text{eff}}-M_G$ -diagram, along with the companions for which an Apsis-Priam estimate of their effective temperature is available⁸, as indicated by the PR1 flag in Table 5. The photometry of all these companions is in good agreement with that expected for main sequence stars.

For the remaining 40 companions their mass and effective temperature are derived from their absolute G-band magnitude by interpolation (inter flag in Table 5) using the M_G -mass- and M_G-T_{eff} -relation from Pecaut and Mamajek (2013), assuming that these companions are main sequence

stars. To test this hypothesis, we compare the obtained effective temperature of the companions either with their Apsis-Priam temperature estimate, if available, or with the effective temperature of the companions inferred from their $(B_p - R_p)$ color and reddening estimate $E(B_p - R_p)$ ⁹, using the $(B_p - R_p)_0-T_{\text{eff}}$ -relation from Pecaut and Mamajek (2013).

For all but three of these companions their effective temperature, determined from their absolute magnitude under the assumption that they are main sequence stars, agrees well with their Apsis-Priam temperature estimate or with the temperature derived from their color. The typical deviation of the different temperature estimates is about 430 K, which is in good agreement with the precision of the derived effective temperatures. We therefore conclude that these companions are all main sequence stars.

In addition, we also compare the Gaia DR3 $(B_p - R_p)$ color of the (C)TOIs and their companions (if any), indicated by the BPRP flag in Table 5. For main sequence companions, fainter/brighter than the (C)TOIs, are expected to appear redder/bluer than the stars, and this is true for most of the detected companions, except for TOI 3714 B, TOI 3984 B, and CTOI 13073396 B. These three companions are also observed with the Panoramic Survey Telescope and Rapid Response System (Pan-STARRS) and their y-, i-, g-band color-composite images are shown in Figure 4. In these images the faint companions are clearly visible as bluish sources next to the associated much brighter (C)TOIs.

The photometric properties of these companions are summarized in Table 1. The companions are several magnitudes fainter than the (C)TOIs but appear bluer than these stars. The temperatures of the companions inferred from their colors are significantly higher (by about 2700 to 6900 K) than the temperatures, derived from their absolute G-band magnitudes, assuming that they are main sequence stars.

⁸As recommended by Andrae et al. (2018), we only use Apsis-Priam temperature estimates in this survey if their flags are equal to 1A000E where A and E can have any value.

⁹The reddening of an object is estimated from its extinction A_G using the relation $A_G/E(B_p - R_p) = 1.89$ from Wang and Chen (2019).

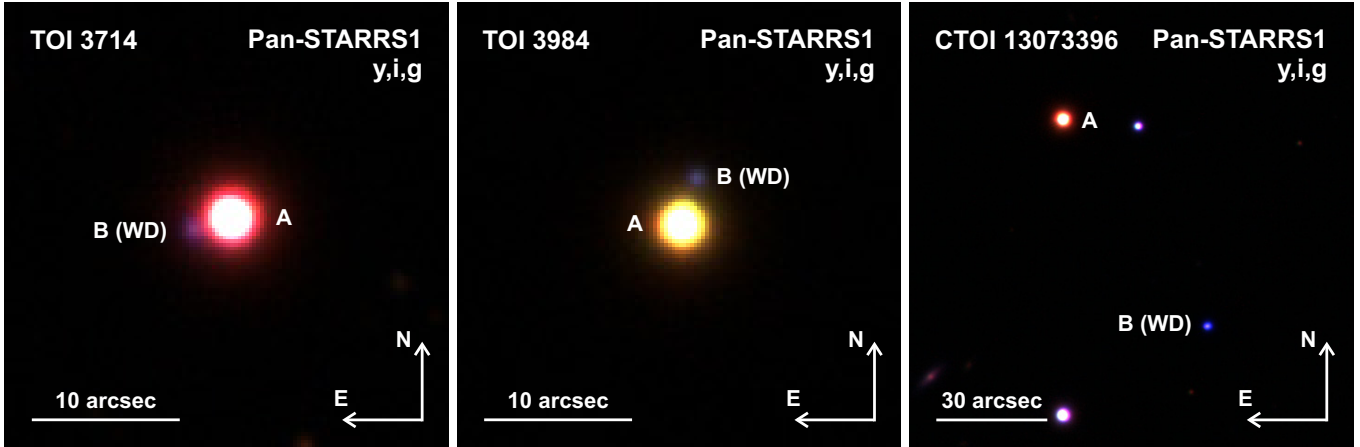


FIGURE 4 (RGB)-color-composite images of TOI3714, TOI3984 and CTOI 13073396 with their white dwarf companions from y-, i- and g-band Pan-STARRS images.

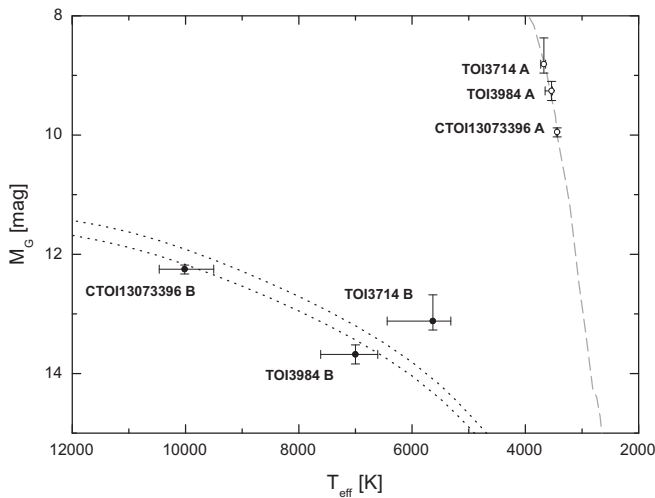


FIGURE 5 $T_{\text{eff}}-M_G$ -diagram of the stellar systems with white dwarf companions detected in this study. The main sequence is shown as a grey dashed line and the evolutionary mass tracks of DA white dwarfs with masses of 0.5 and $0.6 M_{\odot}$ as black dotted lines. The primaries of the systems are plotted as white circles, the white dwarf secondaries as black circles, respectively.

Figure 5 shows these companions together with the other components of their stellar systems in a $T_{\text{eff}}-M_G$ -diagram. For comparison, we plot the main sequence from Pecaut and Mamajek (2013) in this diagram, and the mass tracks for DA white dwarfs from the Bergeron et al. evolutionary models of white dwarfs (for further details see Bédard, Bergeron, Brassard, & Fontaine, 2020; Bergeron et al., 2011; Blouin, Dufour, & Allard, 2018; Holberg & Bergeron, 2006; Kowalski & Saumon, 2006 and Tremblay, Bergeron, & Gianninas,

2011)¹⁰. While the brighter primary components of these systems are all main sequence stars, the faint secondaries are well below the main sequence, and their Gaia photometry best matches that expected for white dwarfs. We therefore conclude that these companions are white dwarfs, as indicated by the WD flag in Table 5.

Another white dwarf companion is revealed in this project due to its intrinsic faintness. TOI 4301 B has an absolute G-band magnitude of $M_G = 13.21^{+0.08}_{-0.1}$ mag and a magnitude difference of $\Delta G = 8.458 \pm 0.005$ mag to the associated potential exoplanet host star TOI 4301 A. Although there is no color information for TOI 4301 B in the Gaia DR3, the white dwarf nature of this companion can be deduced from its photometric properties. While TOI 4301 B is visible in the optical spectral range and is listed in the Gaia DR3, it is not detected in the 2MASS Ks-band image which is shown in Figure 6. In this figure, the expected position of the companion at the 2MASS observing epoch (February 2000) is indicated by a black circle, calculated using the Gaia DR3 astrometry of the companion and the epoch difference between the 2MASS observation and the Gaia DR3 reference epoch (2016.0). The 2MASS image has a $S/N = 10$ detection limit of about 14.9 mag. Near the position of the companion, the star 2MASS 11050267-4602149 ($K_s = 14.6 \pm 0.1$ mag, Skrutskie et al., 2006) is well detected in the 2MASS image, consistent with the given detection limit. If TOI 4301 B were a main sequence star, we would expect its apparent Ks-band magnitude to be $K_s = 14.5 \pm 0.1$ mag, derived from the photometric data of main sequence stars from Pecaut and Mamajek (2013), using the G-band photometry of the companion, the extinction in this band, the given extinction relations $A_G/A_V = 0.789$

¹⁰Online available at: <https://www.astro.umontreal.ca/~bergeron/CoolingModels/>. Version 2021.01.13 is used here.

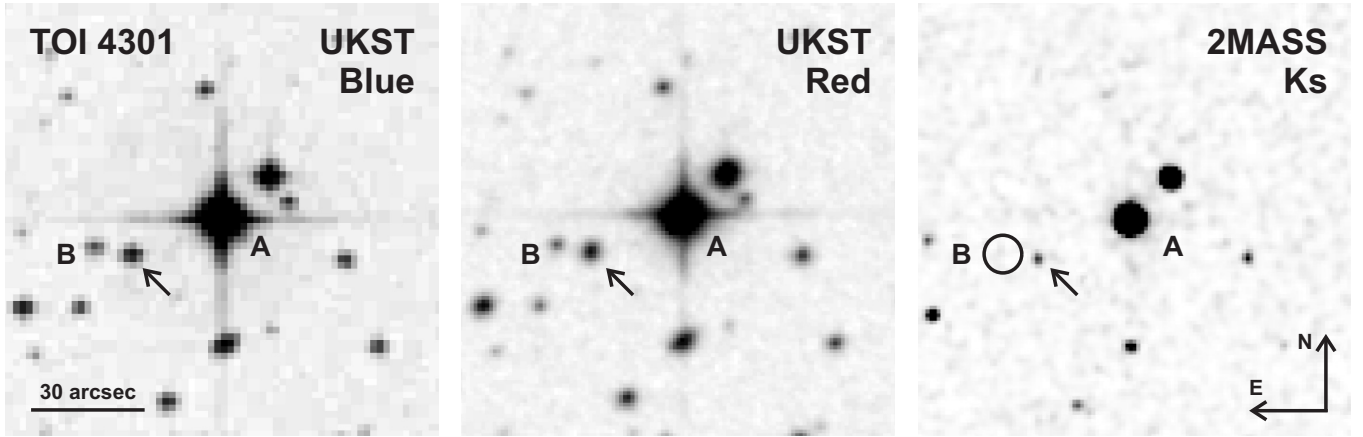


FIGURE 6 TOI 4301 A (center of all images) and its co-moving white dwarf companion TOI 4301 B imaged with the UK Schmidt Telescope (UKST) in the filters GG 395 (Blue) and RG 610 (Red), respectively. The companion is well detected in the blue spectral range, but becomes fainter towards longer wavelengths and is not visible in the 2MASS Ks-band image. The expected position of TOI 4301 B in this image is marked with a black circle. Next to this position is the star 2MASS 11050267-4602149, which is indicated with a black arrow in all images.

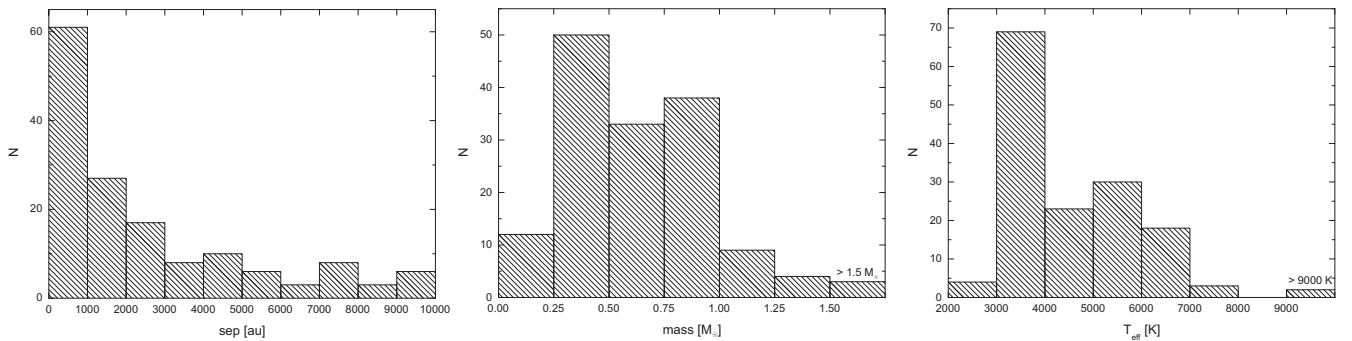


FIGURE 7 The histograms of the properties of the companions detected in this study.

and $A_{K_s}/A_V = 0.078$ from Wang and Chen (2019), and the parallax of TOI 4301. Therefore, if the companion were a main sequence star, it should be clearly visible in the 2MASS image, similar like 2MASS 11050267-4602149. In contrast, if the companion were a white dwarf, we could infer its expected Ks-band photometry as above, but using the evolutionary DA white dwarf models of Bergeron et al. instead. For an assumed companion mass of $0.6 M_\odot$ we obtain $K_s \sim 18.3$ mag, which is clearly below the 2MASS detection limit. We therefore conclude that TOI 4301 B is a white dwarf, due to its intrinsic faintness in the optical and near-infrared spectral range. With the assumed mass of this degenerated companion and the white dwarf evolutionary models mentioned above, the absolute G-band photometry of the companion yields its effective temperature, which is $T_{\text{eff}} = 7447^{+211}_{-158}$ K.

Figure 7 shows the histograms of the properties of all companions detected in this project. The companions have

angular separations to the (C)TOIs, ranging from about 0.4 to 167 arcsec, corresponding to projected separations from 51 up to 9736 au. According to the underlying cumulative distribution function, the frequency of the companions is highest and constant between about 300 and 750 au, decreasing for larger projected separations. Half of all companions have projected separations of less than 1500 au. In total, 5 stellar systems (four binaries, and one hierarchical triples) with projected separations below 200 au are detected, namely: TOI 3073 AB, TOI 3634 AB, TOI 4175 AB+C, TOI 4349 AB, and CTOI 248960573 AB, i.e. the most challenging environments for planet formation identified in this study.

The companion masses range from about 0.11 to $2 M_\odot$ (the mean mass is $\sim 0.6 M_\odot$). The highest companion frequency in the cumulative distribution function is found in the mass range between 0.2 and $0.5 M_\odot$, corresponding to mid to early M dwarfs, according to the relation between mass and spectral type (SpT) from Pecaut and Mamajek (2013). For

higher masses, the companion frequency is lower but constant between about 0.7 and $1.1 M_{\odot}$, from where it decreases continuously towards higher masses. This peak in the companion population is also seen in the distribution of their effective temperature, where the companion frequency is highest at temperatures between about 3200 and 3700 K. There is also a second but weaker clustering of companions between about 4600 and 6100 K, corresponding to mid K to late F-type stars, according to the T_{eff} -SpT-relation from Pecaut and Mamajek (2013).

As can be seen from the separation-mass-diagram in Figure 8, of the 149 companions presented here, 18 are the primary, 124 are the secondary, 5 the tertiary, and 2 the quaternary component of their stellar systems.

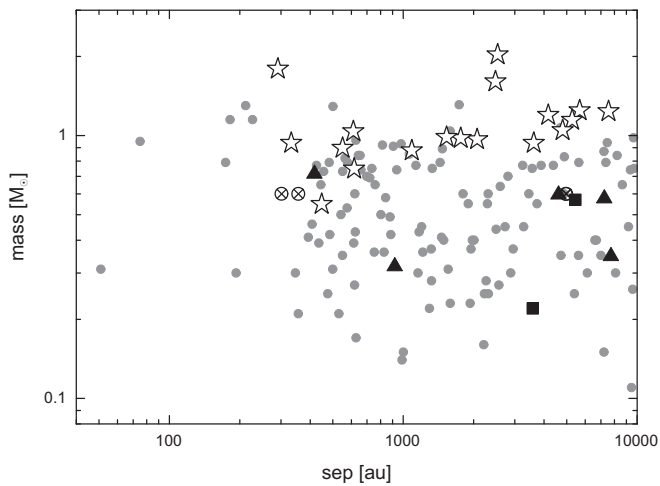


FIGURE 8 The separation-mass-diagram of the companions detected in this study. Companions that are the primary components of their stellar systems are shown as star symbols, secondaries as grey circles, tertiary components as black triangles, and quaternary components as black squares, respectively. Detected white dwarf companions, assumed to have a mass of $0.6 M_{\odot}$, are plotted as white crossed circles (note that the symbols of the white dwarf companions TOI 4301 B, and CTOI 13073396 B overlap at a separation of about 5000 au).

To characterize the detection limit reached in this project, we plot the magnitude difference of all detected companions over their angular separation to the associated (C)TOIs, as shown in Figure 9. For comparison, we plot the Gaia detection limit determined by Mugrauer et al. (2022), which agrees well with the detection limit presented here. Only at small angular separations below about 0.4 arcsec does it seem to be too conservative. In this angular separation range one companion is detected that is about 0.4 mag fainter than the associated TOI.

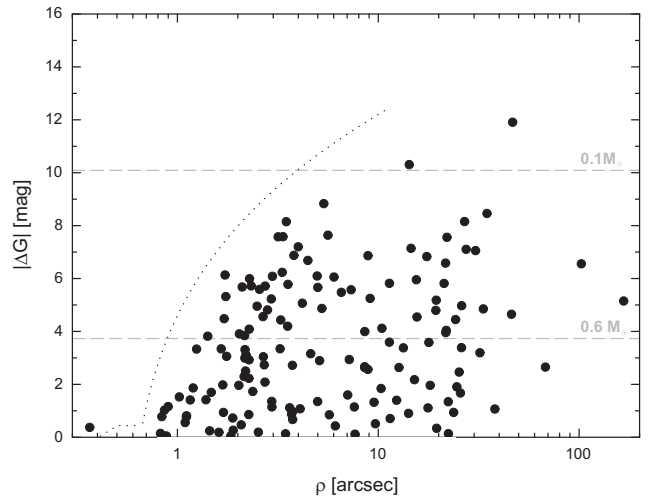


FIGURE 9 The magnitude difference of all detected companions plotted against their angular separation from the associated (C)TOI. The Gaia detection limit, found by Mugrauer et al. (2022), is shown as a dotted line for comparison. The expected average magnitude differences for companions with 0.1 or $0.6 M_{\odot}$ are shown as grey dashed horizontal lines.

The expected brightness difference between the targets of this study and low-mass main sequence companions (shown as grey dashed lines in Figure 9) is estimated using the expected absolute G-band magnitude of these stars, as listed in Pecaut and Mamajek (2013), and the average absolute G-band magnitude of our targets ($M_G \sim 4.2$ mag). As shown in Figure 9, a magnitude difference of about 3.7 mag is reached at an angular separation of about 0.9 arcsec around the targets of this project. This allows the detection of companions with masses down to about $0.6 M_{\odot}$ (mean mass of all detected companions) that are separated from the (C)TOIs by more than 250 au. In addition, companions with masses down to about $0.1 M_{\odot}$ are detectable beyond 4 arcsec, corresponding to a projected separation of 1100 au at the average target distance of 280 pc.

4 | SUMMARY AND OUTLOOK

In recent years, several surveys have been carried out using ground-based observations to explore the multiplicity of exoplanet host stars (see e.g. Ginski, Mugrauer, Adam, Vogt, & van Holstein, 2021; Mugrauer & Ginski, 2015). Here we present the latest results of our survey based on data of the ESA-Gaia mission, which was initiated at the University Observatory Jena in early 2020 with the aim of detecting and characterizing stellar companions of (C)TOIs, i.e. potential exoplanet host stars. In the study presented in this paper we search for companions of 1106 (C)TOIs announced in the

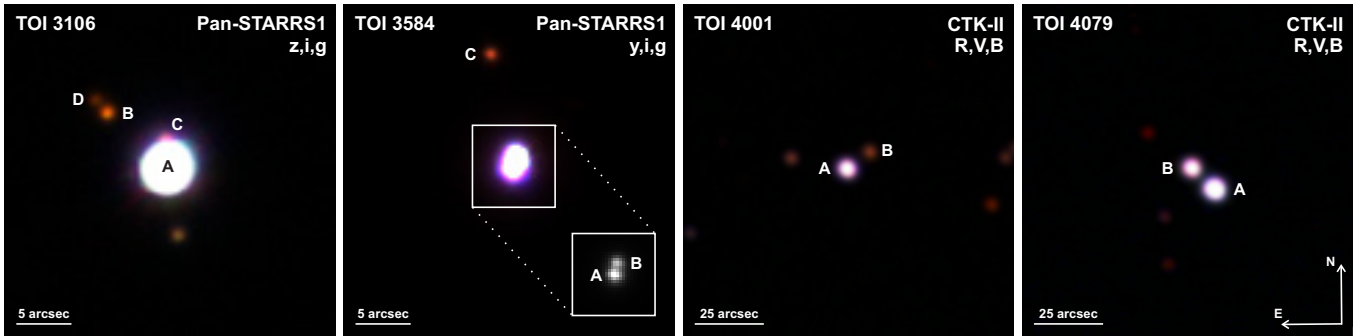


FIGURE 10 (RGB)-color-composite images of the hierarchical quadruple system TOI 3106 AC+BD, and of the triple system TOI 3584 AB+C from z- (or y-), i-, and g-band Pan-STARRS images. A detailed y-band Pan-STARRS image is shown for TOI 3584 AB+C, in which the primary and secondary component of this triple star system are well resolved. The (RGB)-color-composite images of the binary systems TOI 4001 AB, and TOI 4079 BA, are composed of R-, V-, and B-band images taken with the CTK-II at the University Observatory Jena.

(C)TOI release of the ExoFOP-TESS, whose multiplicity has not yet been investigated in the course of our survey, using Gaia DR3 data.

In total, about 33000 sources with accurate astrometric solutions are detected in the Gaia DR3 around 891 targets, while around the remaining 215 targets of this survey no companion-candidates are identified within the applied search radius. In total, new co-moving companions are detected around 142 of all targets whose multiplicity is studied here. In addition, companions around a further 23 (C)TOIs are found in the Gaia DR3, but these had already been detected in the Gaia DR2 by Mugrauer (2019), Mugrauer and Michel (2020), and Michel and Mugrauer (2021). Thus, the multiplicity rate of the investigated (C)TOIs is at least $14.9 \pm 1.1\%$, which is lower than the rate found in our survey so far (e.g. $20.1 \pm 0.9\%$, Mugrauer et al., 2022). The reason for this difference is the low multiplicity rate of the CTOIs examined in this study, which is only about 5%. In contrast, the multiplicity rate of the TOIs is $19.9 \pm 1.5\%$, which is well in line with the multiplicity rates found earlier in our survey. As described above, the CTOIs whose multiplicity is studied here are closer to the Sun than the TOIs. A smaller distance usually leads to higher proper motion, brightness and angular separation of potential companions, which should facilitate their detection. Therefore, the surprisingly low multiplicity rate of the CTOIs found in this study must be an effect of the target selection by the ExoFOP-TESS.

Color-composite images of some of the detected stellar systems are shown in Figure 10, taken with Pan-STARRS or with the Cassegrain-Teleskop-Kamera (CTK-II, Mugrauer, 2016) at the University Observatory Jena. In addition to 134 binaries, two quadruple star systems are revealed in which the (C)TOIs have both a close companion and a distant binary

companion. Furthermore, three hierarchical triple star systems are detected, whose individual components are listed in the Gaia DR3. Moreover, significant ($Mdn(sig) = 20$) astrometric non-single-star solutions are listed in the Gaia DR3 for the co-moving companions of TOI 3875, TOI 4128, and TOI 4420 (indicated with the NSS flag in Table 5). For the companions of TOI 3875 and TOI 4128, a Keplerian orbital motion of their photocenter is detected in the Gaia astrometry ($P = 502.5 \pm 5.0$ days, $a = 0.99 \pm 0.05$ mas, $e = 0.36 \pm 0.10$, $i = 86.9 \pm 2.5^\circ$ for TOI 3875 B, and $P = 802.7 \pm 11.2$ days, $a = 1.86 \pm 0.03$ mas, $e = 0.61 \pm 0.02$, $i = 129.1 \pm 1.2^\circ$ for TOI 4128 B, respectively). So these companions are themselves close binary systems. With the masses of TOI 3875 B and TOI 4128 B, and their Gaia DR3 parallaxes redetermined in the non-single star solutions ($\pi = 2.482 \pm 0.026$ mas for TOI 3875 B, and $\pi = 3.210 \pm 0.017$ mas for TOI 4128 B, respectively), the masses of the unseen tertiary components and the semi-major axis of these close binary systems can be determined. We obtain $0.37 \pm 0.03 M_\odot$ for the mass of TOI 3875 C, and $0.38 \pm 0.02 M_\odot$ for TOI 4128 C, respectively. The semi-major axis of the TOI 3875 BC system is $a = 1.33 \pm 0.03$ au, which corresponds to about 3 mas at the distance of the system, and $a = 1.78 \pm 0.05$ au (~ 6 mas) for TOI 4128 BC, respectively. The companion of TOI 4420 is identified as a single-lined spectroscopic binary in the Gaia DR3. According to its significant ($sig = 12$) orbital solution, the companion has a radial velocity (RV) semi-amplitude of $K = 20.9 \pm 1.8$ km/s, a period of $P = 4.7257 \pm 0.0009$ days, and an eccentricity of $e = 0.24 \pm 0.09$. Together with the mass of TOI 4420 B this gives the minimum-mass of the unresolved companion TOI 4420 C ($\sim 0.16 M_\odot$), and the minimum of the semi-major axis of this close binary system (~ 0.05 au). Thus, TOI 3875, TOI 4128, and TOI 4420 are three more hierarchical

triples composed of the TOIs and their distant binary companions. Hence, a total of 6 hierarchical triple star systems are detected in the multiplicity study presented here.

Furthermore, the companion TOI 3956 A, is listed in the Gaia DR3 as having a significant acceleration of its proper motion ($\dot{\mu} = 1.22 \pm 0.04 \text{ mas/yr}^2$), i.e. this star probably has an additional close stellar companion with an orbital period longer than the 34-months period on which the Gaia DR3 is based on. We therefore classify TOI 3956 as a potential hierarchical triple star system, whose triple nature will have to be confirmed by follow-up observations.

As expected for components of stellar systems the (C)TOIs and the detected companions are equidistant and share a common proper motion, as verified by their accurate Gaia DR3 parallax and proper motion. In particular, the direct proof of the equidistance of the individual components of the stellar systems, as done in this study by comparing their parallax, was not possible in previous multiplicity surveys prior to the release of the precise Gaia data, because in particular for most of the faint companions their parallax could not be measured by the ESA-Hipparcos mission (Perryman et al., 1997).

However, 23 companions identified in this project are already listed in the WDS, either as co-moving companions or as companion-candidates of the (C)TOIs, requiring confirmation of their companionship, which is finally provided by this study. Although the WDS is currently the most complete catalog of multiple star systems available, containing relative astrometric measurements of multiple star systems over a period of more than 300 years, 126 (i.e. about 84 % of all) companions not listed in the WDS are detected in this project and are marked with the \star flag in Table 4. This demonstrates the great potential of the ESA-Gaia mission for the study of stellar multiplicity, especially for the detection of wide companions, as shown by the derived detection limit of this study in Figure 9. On average, all stellar companions with masses down to about $0.1 M_{\odot}$ are detectable around the targets in this study beyond about 4 arcsec (or 1100 au of projected separation), and more than half of all detected companions have such separations. Overall, companions with projected separations between about 50 and 9700 au are detected, and the frequency of companions is constant and highest for separations between about 300 and 750 au, while it decreases significantly for larger projected separations. The companions found in this project have masses ranging from about 0.11 to $2 M_{\odot}$ and are most abundant in the mass range between 0.2 and $0.5 M_{\odot}$. In addition to main sequence stars, four white dwarfs are identified as co-moving companions of the (C)TOIs, whose true nature is revealed based on their photometric properties.

A significant ($sig\text{-}\mu_{\text{rel}} \geq 3$) differential proper motion μ_{rel} relative to the associated (C)TOIs is detected for 122 (i.e. about 80 % of all) companions presented here. We derive the

escape velocity μ_{esc} of all these companions using the approximation described in Mugrauer (2019). The differential proper motion of most of these companions is consistent with orbital motion. In contrast, the differential proper motion of 19 companions significantly exceeds the expected escape velocity. Since these companions all have a high degree of common proper motion ($cpm\text{-}index \geq 10$), this may indicate a higher degree of multiplicity as described in Mugrauer (2019). In fact, five of the companions are members of already confirmed hierarchical triple or quadruple star systems. For the companion TOI 3956 A, a significant acceleration of its proper motion is listed in the Gaia DR3, indicating that this star is itself a close binary, i.e. TOI 3956 is a potential hierarchical triple star system. Follow-up (high contrast imaging) observations are needed to further investigate the multiple status of all these particular systems and their companions, which are summarized in Table 2.

TABLE 2 List of all detected companions (sorted by their identifier) whose differential proper motion μ_{rel} relative to the (C)TOIs significantly exceeds the expected escape velocity μ_{esc} . Companions already known to be members of hierarchical triple or quadruple star systems are labelled with $\star\star\star$ or $\star\star\star\star$, those in potential triple star systems with $(\star\star\star)$, respectively.

Companion	μ_{rel} [mas/yr]	μ_{esc} [mas/yr]	
TOI 2690 D	2.41 ± 0.06	0.66 ± 0.04	$\star\star\star\star$
TOI 2774 B	1.07 ± 0.10	0.34 ± 0.01	
TOI 2816 A	0.49 ± 0.02	0.36 ± 0.02	
TOI 3039 B	3.72 ± 0.35	0.23 ± 0.01	
TOI 3106 B	7.69 ± 0.17	0.48 ± 0.01	$\star\star\star\star$
TOI 3106 D	7.91 ± 0.36	0.41 ± 0.01	$\star\star\star\star$
TOI 3314 B	1.08 ± 0.11	0.55 ± 0.05	
TOI 3353 B	2.67 ± 0.04	1.42 ± 0.05	
TOI 3560 B	1.28 ± 0.14	0.40 ± 0.02	
TOI 3628 C	2.09 ± 0.33	0.39 ± 0.02	$\star\star\star$
TOI 3682 B	5.32 ± 0.05	0.32 ± 0.02	
TOI 3781 B	1.33 ± 0.04	0.67 ± 0.01	
TOI 3829 B	3.00 ± 0.11	1.25 ± 0.05	
TOI 3889 B	1.92 ± 0.03	1.36 ± 0.03	
TOI 3956 A	1.18 ± 0.03	0.67 ± 0.02	$(\star\star\star)$
TOI 4021 B	1.00 ± 0.02	0.35 ± 0.01	
TOI 4175 C	4.50 ± 0.05	2.49 ± 0.09	$\star\star\star$
TOI 4179 A	6.14 ± 0.25	1.92 ± 0.10	
TOI 4370 B	1.08 ± 0.09	0.65 ± 0.03	

In addition to astrometry, also RV data can be used to check the companionship of the components of stellar systems. For common proper motion pairs, we do not expect significant differences between the RVs of their components, since their orbital motion (especially for wide ones) around their barycenter is typically much smaller than the systematic velocity. For 59 companions detected in this study (i.e. less than 40% of all) a comparison between their RV and that of the associated (C)TOI is possible in the Gaia DR3. As expected, the RVs of most of these companions and the (C)TOIs do not significantly deviate from each other. Only four companions have significant RV deviations, namely: TOI 3956 A (8.35 ± 2.70 km/s), TOI 4175 B (1.98 ± 0.60 km/s), TOI 4179 A (2.34 ± 0.36 km/s), and TOI 4420 B (14.99 ± 4.01 km/s). This may indicate the presence of additional close stellar companions in these systems that induce faster orbital motions. This is particularly the case for companions, belonging to stellar systems whose components have a high degree of common proper motion, as is the case for the four companions mentioned above (*cpm-index* ≥ 16). The companions TOI 3956 A, and TOI 4420 B both have non-single star solutions in the Gaia DR3, so are themselves close binary systems. TOI 4175 B is a member of a hierarchical triple star system whose components are resolved by Gaia, and TOI 4179 A is a member of a potential triple star system according to its Gaia DR3 astrometry.

As demonstrated with the target sample studied here, even in the latest data release of the ESA-Gaia mission, RVs are available for only a minority of the detected companions. For this reason, we do not use RV data for companionship verification in this survey so far, but will include it as soon as it is available for most of the detected companions, which is expected for the upcoming Gaia data releases.

The survey, whose latest results are presented here, is an ongoing project whose target list is continually growing as a result of the ongoing analysis of photometric data collected by the TESS mission. The multiplicity of all these newly detected (C)TOIs will be explored in the course of this survey, and the detected companions and their determined properties will be reported regularly in this journal and also published online in the VizieR database (Ochsenbein, Bauer, & Marcout, 2000)¹¹, and on the website of this survey¹². The results of this survey, combined with those of high-contrast imaging observations of the (C)TOIs, which can detect close companions with projected separations down to only a few au, will complete our knowledge of the multiplicity of all these potential exoplanet host stars.

REFERENCES

- Anders, F., Khalatyan, A., Chiappini, C. et al. (2019, August), *A&A*, 628, A94.
- Anders, F., Khalatyan, A., Queiroz, A. B. A. et al. (2022, February), *A&A*, 658, A91.
- Andrae, R., Fouesneau, M., Creevey, O. et al. (2018, August), *A&A*, 616, A8.
- Bédard, A., Bergeron, P., Brassard, P., & Fontaine, G. (2020, October), *ApJ*, 901(2), 93.
- Bergeron, P., Wesemael, F., Dufour, P. et al. (2011, August), *ApJ*, 737(1), 28.
- Blouin, S., Dufour, P., & Allard, N. F. (2018, August), *ApJ*, 863(2), 184.
- Gaia Collaboration, Brown, A. G. A., Vallenari, A. et al. (2018, August), *A&A*, 616, A1.
- Gaia Collaboration, Brown, A. G. A., Vallenari, A. et al. (2021, May), *A&A*, 649, A1.
- Gaia Collaboration, Vallenari, A., Brown, A. G. A. et al. (2022, July), *arXiv e-prints*, arXiv:2208.00211.
- Ginski, C., Mugrauer, M., Adam, C., Vogt, N., & van Holstein, R. G. (2021, May), *A&A*, 649, A156. doi:
- Holberg, J. B., & Bergeron, P. (2006, September), *AJ*, 132, 1221.
- Kowalski, P. M., & Saumon, D. (2006, November), *ApJL*, 651, L137.
- Michel, K. U., & Mugrauer, M. (2021, March), *FrASS*, 8, 14.
- Mugrauer, M. (2016, March), *Astronomische Nachrichten*, 337(3), 226-234.
- Mugrauer, M. (2019, December), *MNRAS*, 490(4), 5088.
- Mugrauer, M., & Ginski, C. (2015, July), *MNRAS*, 450(3), 3127-3136. doi:
- Mugrauer, M., & Michel, K.-U. (2020, December), *Astronomische Nachrichten*, 341(10), 996-1030.
- Mugrauer, M., & Michel, K.-U. (2021, July), *Astronomische Nachrichten*, 342(6), 840-864.
- Mugrauer, M., Zander, J., & Michel, K.-U. (2022, July), *Astronomische Nachrichten*, 343, e24017. doi:
- Ochsenbein, F., Bauer, P., & Marcout, J. (2000, April), *A&AS*, 143, 23.
- Pecaut, M. J., & Mamajek, E. E. (2013, September), *ApJS*, 208, 9.
- Perryman, M. A. C., Lindgren, L., Kovalevsky, J. et al. (1997, July), *A&A*, 500, 501-504.
- Ricker, G. R., Winn, J. N., Vanderspek, R. et al. (2015, January), *JATIS*, 1, 014003.
- Schneider, J., Dedieu, C., Le Sidaner, P., Savalle, R., & Zolotukhin, I. (2011, August), *A&A*, 532, A79.
- Skrutskie, M. F., Cutri, R. M., Stiening, R. et al. (2006, February), *AJ*, 131(2), 1163-1183.
- Tremblay, P.-E., Bergeron, P., & Gianninas, A. (2011, April), *ApJ*, 730, 128.
- Wang, S., & Chen, X. (2019, June), *ApJ*, 877(2), 116.



¹¹Online available at: <https://vizier.u-strasbg.fr/viz-bin/VizieR>

¹²Online available at: [https://www.astro.uni-jena.de/Users/markus/Multiplicity_of_\(C\)TOIs.html](https://www.astro.uni-jena.de/Users/markus/Multiplicity_of_(C)TOIs.html)

ACKNOWLEDGMENTS

We used data from:

(1) the European Space Agency (ESA) mission Gaia (<https://www.cosmos.esa.int/gaia>), processed by the Gaia Data Processing and Analysis Consortium (DPAC, <https://www.cosmos.esa.int/web/gaia/dpac/consortium>). The DPAC is funded by national institutions, in particular those participating in the Gaia Multilateral Agreement.

(2) the Exoplanet Follow-up Observing Program website, operated by the California Institute of Technology, on behalf of the National Aeronautics and Space Administration under the Exoplanet Exploration Program.

(3) the Simbad and VizieR databases operated at the CDS in Strasbourg, France.

(4) the Extrasolar Planets Encyclopaedia.

(5) the Pan-STARRS1 surveys, made possible by contributions from the Institute for Astronomy, the University of Hawaii, the Pan-STARRS Project Office, the Max-Planck Society and its participating institutes, the Max Planck Institute for Astronomy, Heidelberg and the Max Planck Institute for Extraterrestrial Physics, Garching, The Johns Hopkins University, Durham University, the University of Edinburgh, the Queen's University Belfast, the Harvard-Smithsonian Center for Astrophysics, the Las Cumbres Observatory Global Telescope Network Incorporated, the National Central University of Taiwan, the Space Telescope Science Institute, and the National Aeronautics and Space Administration under Grant No. NNX08AR22G issued through the Planetary Science Division of the NASA Science Mission Directorate, the National Science Foundation Grant No. AST-1238877, the University of Maryland, Eotvos Lorand University (ELTE), and the Los Alamos National Laboratory. The Pan-STARRS1 Surveys are archived at the Space Telescope Science Institute (STScI) and are available through MAST, the Mikulski Archive for Space Telescopes. Additional support for the Pan-STARRS1 public science archive is provided by the Gordon and Betty Moore Foundation.

(6) the Second Palomar Observatory Sky Survey (POSS-II), made by the California Institute of Technology with funds from the National Science Foundation, the National Geographic Society, the Sloan Foundation, the Samuel Oschin Foundation, and the Eastman Kodak Corporation. The UK Schmidt Telescope was operated by the Royal Observatory Edinburgh, with funding from the UK Science and Engineering Research Council (later the UK Particle Physics and Astronomy Research Council), until 1988 June, and thereafter by the Anglo-Australian Observatory. The blue plates of the southern Sky Atlas and its Equatorial Extension (together known as the SERC-J), as well as the Equatorial Red (ER),

and the Second Epoch [red] Survey (SES) were all taken with the UK Schmidt. Supplemental funding for sky-survey work at the ST ScI is provided by the European Southern Observatory. The Digitized Sky Surveys were produced at the Space Telescope Science Institute under U.S. Government grant NAG W-2166. The images of these surveys are based on photographic data obtained using the Oschin Schmidt Telescope on Palomar Mountain and the UK Schmidt Telescope. The plates were processed into the present compressed digital form with the permission of these institutions.

(7) the Two Micron All Sky Survey, a joint project of the University of Massachusetts and the Infrared Processing and Analysis Center/California Institute of Technology, funded by the National Aeronautics and Space Administration and the National Science Foundation.

(8) the University Observatory Jena, which is operated by the Astrophysical Institute of the Friedrich-Schiller-University.



TABLE 3 This table summarizes for all (C)TOIs (listed first) and their detected co-moving companions their Gaia DR3 parallax π , proper motion μ in right ascension and declination, astrometric excess noise $epsi$, G-band magnitude, as well as the used Apsis-Prism G-Band extinction estimate A_G or if not available the G-Band extinction, listed in the SHC.

TOI	π [mas]	$\mu_\alpha \cos(\delta)$ [mas/yr]	μ_δ [mas/yr]	$epsi$ [mas]	G [mag]	A_G [mag]	
2689 A	3.1299 ± 0.0125	5.403 ± 0.013	-27.899 ± 0.014	0.000	13.2169 ± 0.0028		
2689 B	3.1764 ± 0.0394	5.407 ± 0.041	-28.029 ± 0.043	0.000	16.1522 ± 0.0028	$0.8067^{+0.3850}_{-0.2357}$	
2690 B	4.5220 ± 0.0200	10.420 ± 0.024	-8.449 ± 0.020	0.126	11.6878 ± 0.0028	$0.0190^{+0.2290}_{-0.0110}$	
2690 A	4.5704 ± 0.0175	10.378 ± 0.019	-8.891 ± 0.017	0.098	10.0158 ± 0.0028	$0.7493^{+0.2668}_{-0.2786}$	
2690 C	4.6961 ± 0.0299	11.071 ± 0.032	-7.888 ± 0.032	0.185	12.4131 ± 0.0035		
2690 D	4.4724 ± 0.0487	12.827 ± 0.050	-8.404 ± 0.047	0.353	13.5936 ± 0.0029		
2713 A	4.0423 ± 0.0125	-15.172 ± 0.011	-14.971 ± 0.011	0.000	13.0583 ± 0.0028	$0.1872^{+0.0938}_{-0.1692}$	
2713 B	4.0369 ± 0.0489	-15.679 ± 0.044	-15.446 ± 0.044	0.000	16.3996 ± 0.0030		
2774 A	1.9516 ± 0.0692	-7.016 ± 0.057	-2.619 ± 0.050	0.585	13.2880 ± 0.0029		
2774 B	1.9328 ± 0.0957	-8.056 ± 0.081	-2.374 ± 0.070	0.753	15.9220 ± 0.0031	$1.3389^{+0.1013}_{-0.1013}$	SHC
2803 A	2.0234 ± 0.0117	0.749 ± 0.009	11.908 ± 0.011	0.073	12.4168 ± 0.0028		
2803 B	2.0241 ± 0.0119	0.795 ± 0.009	11.972 ± 0.011	0.066	12.7534 ± 0.0028	$0.0260^{+0.0950}_{-0.0220}$	
2816 B	1.9855 ± 0.0138	18.981 ± 0.015	1.137 ± 0.016	0.063	13.9355 ± 0.0028		
2816 A	2.0217 ± 0.0092	18.496 ± 0.009	1.112 ± 0.010	0.000	12.6136 ± 0.0028	$1.6313^{+0.1550}_{-0.2834}$	
2892 A	2.6068 ± 0.0137	-8.416 ± 0.017	6.244 ± 0.019	0.009	13.9810 ± 0.0028	$0.2410^{+0.0738}_{-0.1176}$	
2892 B	2.7029 ± 0.0414	-7.484 ± 0.058	6.334 ± 0.058	0.382	15.1238 ± 0.0029		
2909 A	1.8407 ± 0.1081	-10.374 ± 0.097	3.687 ± 0.120	1.189	11.5362 ± 0.0028	$0.8720^{+0.0700}_{-0.0951}$	
2909 B	1.3577 ± 0.0555	-10.198 ± 0.047	3.328 ± 0.063	0.547	14.2692 ± 0.0028		
2911 A	5.5605 ± 0.0220	-32.895 ± 0.024	39.756 ± 0.025	0.054	15.3347 ± 0.0029		
2911 B	5.5101 ± 0.0423	-33.121 ± 0.046	39.720 ± 0.054	0.347	16.1902 ± 0.0028	$1.1278^{+0.4704}_{-0.4704}$	SHC
2956 A	2.7756 ± 0.0123	14.483 ± 0.014	-5.685 ± 0.014	0.081	12.9223 ± 0.0028	$0.0951^{+0.1019}_{-0.0951}$	SHC
2956 B	2.8875 ± 0.0994	14.348 ± 0.120	-5.420 ± 0.115	0.154	18.1029 ± 0.0031		
3039 A	2.2584 ± 0.0142	-22.097 ± 0.017	7.596 ± 0.018	0.124	12.9689 ± 0.0028	$0.3960^{+0.1411}_{-0.1140}$	
3039 B	2.0635 ± 0.2918	-23.398 ± 0.326	4.107 ± 0.348	0.856	19.5510 ± 0.0045		
3040 A	2.1777 ± 0.0084	-29.827 ± 0.010	15.771 ± 0.010	0.031	12.6178 ± 0.0028		
3040 B	2.1904 ± 0.0099	-29.960 ± 0.012	15.665 ± 0.012	0.072	12.7458 ± 0.0028	$0.2197^{+0.1653}_{-0.0822}$	
3073 A	16.0192 ± 0.0633	-42.316 ± 0.046	-82.667 ± 0.068	0.566	12.9160 ± 0.0029		
3073 B	16.2470 ± 0.0967	-37.439 ± 0.048	-87.657 ± 0.116	0.474	13.0601 ± 0.0032	$0.0000^{+0.0543}_{-0.0000}$	SHC
3097 A	2.4078 ± 0.0184	-16.449 ± 0.013	25.469 ± 0.014	0.068	13.7774 ± 0.0028		
3097 B	2.4004 ± 0.0375	-16.803 ± 0.035	25.317 ± 0.040	0.086	15.1920 ± 0.0045	$0.0000^{+0.3472}_{-0.0000}$	SHC
3106 A	2.4846 ± 0.0375	-34.590 ± 0.041	-6.137 ± 0.030	0.283	12.4863 ± 0.0028		
3106 B	2.1856 ± 0.1414	-42.201 ± 0.164	-5.029 ± 0.117	0.303	18.0587 ± 0.0033		
3106 C	2.5911 ± 0.2775	-35.221 ± 0.346	-6.048 ± 0.376	0.502	18.4780 ± 0.0079		
3106 D	2.3662 ± 0.3323	-42.467 ± 0.356	-5.403 ± 0.274	0.525	19.3475 ± 0.0045		
3155 A	4.9802 ± 0.0118	-30.047 ± 0.008	2.360 ± 0.010	0.054	12.2016 ± 0.0029	$0.4635^{+0.2566}_{-0.1975}$	
3155 B	4.9645 ± 0.0637	-30.140 ± 0.047	2.263 ± 0.053	0.056	17.0518 ± 0.0028		
3159 A	2.3238 ± 0.0126	14.274 ± 0.010	-7.779 ± 0.012	0.078	11.7695 ± 0.0028		
3159 B	2.2756 ± 0.0596	14.337 ± 0.052	-7.802 ± 0.065	0.194	16.8338 ± 0.0030	$1.1801^{+0.4039}_{-0.4039}$	SHC
3179 A	2.2367 ± 0.0192	-13.150 ± 0.022	16.482 ± 0.022	0.184	12.6238 ± 0.0028		
3179 B	2.2209 ± 0.0626	-14.335 ± 0.111	16.021 ± 0.045	0.186	14.1466 ± 0.0030	$0.0000^{+0.4931}_{-0.0000}$	SHC
3202 A	2.6257 ± 0.0196	-17.827 ± 0.021	-10.501 ± 0.019	0.125	12.8707 ± 0.0028	$0.6382^{+0.1162}_{-0.1162}$	SHC
3202 B	2.7703 ± 0.1460	-17.690 ± 0.173	-10.641 ± 0.138	0.151	18.3475 ± 0.0032		
3205 A	4.0476 ± 0.0440	-131.821 ± 0.049	-35.458 ± 0.038	0.278	14.3176 ± 0.0028	$0.3053^{+0.4982}_{-0.2789}$	
3205 B	3.9962 ± 0.0782	-130.496 ± 0.089	-35.008 ± 0.067	0.409	16.2783 ± 0.0036		
3250 A	2.3659 ± 0.0218	-27.450 ± 0.023	9.163 ± 0.021	0.041	12.5500 ± 0.0028		
3250 B	2.4710 ± 0.1478	-27.086 ± 0.140	8.708 ± 0.147	0.677	14.8428 ± 0.0031	$1.4263^{+0.3198}_{-0.4411}$	

TABLE 3 continued

TOI	π [mas]	$\mu_\alpha \cos(\delta)$ [mas/yr]	μ_δ [mas/yr]	ϵ [mas]	G [mag]	A_G [mag]	
3252 A	3.6369 ± 0.0171	-47.791 ± 0.018	-46.007 ± 0.019	0.064	13.0062 ± 0.0028		
3252 B	3.6551 ± 0.0208	-47.701 ± 0.022	-46.008 ± 0.024	0.049	13.9073 ± 0.0028	$0.5420^{+0.3447}_{-0.1705}$	
3266 A	1.9643 ± 0.0269	13.758 ± 0.033	4.392 ± 0.029	0.295	12.7626 ± 0.0028		
3266 B	1.9978 ± 0.0184	13.303 ± 0.037	4.516 ± 0.028	0.100	13.5277 ± 0.0028	$0.0000^{+0.4945}_{-0.0000}$	SHC
3277 A	3.6645 ± 0.0145	36.441 ± 0.011	-117.552 ± 0.010	0.000	13.3531 ± 0.0028		
3277 B	3.7431 ± 0.0658	36.204 ± 0.050	-117.525 ± 0.047	0.335	16.2788 ± 0.0033	$1.7400^{+0.4530}_{-0.4530}$	SHC
3284 A	2.0513 ± 0.0454	-2.842 ± 0.044	3.096 ± 0.035	0.371	11.3851 ± 0.0028	$0.1411^{+0.1729}_{-0.1411}$	SHC
3284 B	2.2253 ± 0.2558	-2.887 ± 0.309	2.973 ± 0.250	0.659	18.5826 ± 0.0149		
3288 A	4.9687 ± 0.0248	-6.566 ± 0.022	-20.080 ± 0.014	0.041	14.2346 ± 0.0028	$1.0060^{+0.1690}_{-0.3141}$	
3288 B	5.3843 ± 0.1201	-6.719 ± 0.114	-20.952 ± 0.073	0.450	17.2239 ± 0.0031		
3294 A	2.8964 ± 0.0205	7.488 ± 0.017	-6.949 ± 0.014	0.137	12.2883 ± 0.0028	$1.0358^{+0.4293}_{-0.4805}$	
3294 B	3.0028 ± 0.0205	7.605 ± 0.017	-7.933 ± 0.015	0.132	12.5503 ± 0.0047		
3314 A	1.8765 ± 0.0428	5.630 ± 0.046	-4.350 ± 0.042	0.309	13.0442 ± 0.0032	$0.5955^{+0.2416}_{-0.1916}$	
3314 B	2.0938 ± 0.0866	6.610 ± 0.098	-4.803 ± 0.086	0.176	17.1279 ± 0.0038		
3342 B	2.9571 ± 0.0142	-9.769 ± 0.013	-24.855 ± 0.011	0.057	12.3031 ± 0.0028		
3342 A	2.8911 ± 0.0246	-9.779 ± 0.022	-24.778 ± 0.020	0.150	10.9629 ± 0.0028	$0.3310^{+0.2686}_{-0.2071}$	
3344 A	4.0494 ± 0.0289	-9.860 ± 0.029	-3.521 ± 0.021	0.077	11.4234 ± 0.0028		
3344 B	4.0057 ± 0.0481	-8.921 ± 0.046	-3.676 ± 0.029	0.117	14.5398 ± 0.0030	$0.0000^{+0.3096}_{-0.0000}$	SHC
3353 A	12.6836 ± 0.0105	-5.941 ± 0.013	38.620 ± 0.013	0.059	9.2522 ± 0.0034		
3353 B	12.6756 ± 0.0319	-8.591 ± 0.040	38.947 ± 0.042	0.171	15.8066 ± 0.0029	$0.7513^{+0.3138}_{-0.2249}$	
3355 A	3.7893 ± 0.0141	12.255 ± 0.018	37.028 ± 0.019	0.100	11.1883 ± 0.0028	$0.0090^{+0.1485}_{-0.0090}$	
3355 B	3.4693 ± 0.0994	12.573 ± 0.127	37.110 ± 0.155	0.441	16.9064 ± 0.0043		
3386 A	1.9732 ± 0.0270	-3.972 ± 0.027	-0.951 ± 0.030	0.283	12.9104 ± 0.0028	$0.2950^{+0.1130}_{-0.1211}$	
3386 B	1.5039 ± 0.3109	-3.630 ± 0.280	-1.099 ± 0.339	0.583	19.5938 ± 0.0063		
3398 A	6.0119 ± 0.0164	39.572 ± 0.018	-59.047 ± 0.012	0.097	12.8762 ± 0.0028	$0.1690^{+0.1623}_{-0.1071}$	
3398 B	5.8215 ± 0.2057	39.506 ± 0.227	-60.221 ± 0.155	0.679	18.9304 ± 0.0039		
3444 A	2.0369 ± 0.0169	-9.773 ± 0.017	-6.666 ± 0.013	0.101	12.4612 ± 0.0028	$1.0403^{+0.2006}_{-0.1879}$	
3444 B	1.9657 ± 0.5421	-7.917 ± 0.564	-6.394 ± 0.487	0.474	20.0347 ± 0.0155		
3450 A	3.8886 ± 0.0499	-18.362 ± 0.042	-14.793 ± 0.055	0.356	11.7634 ± 0.0028		
3450 B	3.3865 ± 0.0670	-18.130 ± 0.061	-16.052 ± 0.084	0.514	11.8100 ± 0.0030		
3490 B	3.6770 ± 0.0098	-19.944 ± 0.013	12.563 ± 0.011	0.000	13.2023 ± 0.0028		
3490 A	3.6705 ± 0.0102	-19.247 ± 0.013	11.830 ± 0.012	0.081	12.0595 ± 0.0028	$0.3050^{+0.2115}_{-0.1521}$	
3491 A	1.8445 ± 0.1476	-8.101 ± 0.190	-14.372 ± 0.134	1.257	12.6121 ± 0.0029		
3491 B	1.7043 ± 0.0225	-7.265 ± 0.026	-14.492 ± 0.021	0.000	14.7859 ± 0.0028	$0.3670^{+0.2306}_{-0.2478}$	
3492 A	4.9324 ± 0.0137	-8.903 ± 0.016	-1.924 ± 0.015	0.094	8.8301 ± 0.028	$0.2360^{+0.2513}_{-0.2360}$	SHC
3492 B	4.0531 ± 1.2172	-8.824 ± 1.703	-1.747 ± 1.531	2.199	20.7374 ± 0.0123		
3500 A	5.1961 ± 0.0275	-58.420 ± 0.028	-38.469 ± 0.025	0.201	11.3464 ± 0.0028	$0.3050^{+0.2660}_{-0.1344}$	
3500 B	5.2136 ± 0.0277	-56.720 ± 0.030	-39.769 ± 0.026	0.158	14.0653 ± 0.0028		
3503 B	2.2555 ± 0.0162	-14.127 ± 0.019	-1.361 ± 0.016	0.145	10.4002 ± 0.0028		
3503 A	2.2162 ± 0.0257	-15.004 ± 0.030	-1.096 ± 0.026	0.270	9.5537 ± 0.028	$0.3590^{+0.0716}_{-0.1691}$	
3504 B	3.3547 ± 0.0116	4.594 ± 0.008	-10.666 ± 0.011	0.062	12.0330 ± 0.0031		
3504 A	3.3862 ± 0.0127	4.657 ± 0.009	-10.577 ± 0.012	0.084	10.9256 ± 0.0028	$0.7582^{+0.4521}_{-0.3753}$	
3514 A	2.3913 ± 0.0117	5.950 ± 0.011	13.680 ± 0.012	0.000	13.4043 ± 0.0028	$0.1790^{+0.2678}_{-0.1314}$	
3514 B	2.4018 ± 0.0632	5.398 ± 0.058	13.328 ± 0.077	0.416	16.4625 ± 0.0032		
3522 A	2.6061 ± 0.0112	-5.315 ± 0.011	-6.051 ± 0.012	0.000	13.4646 ± 0.0028		
3522 B	2.6225 ± 0.0139	-5.170 ± 0.014	-5.927 ± 0.015	0.000	14.1333 ± 0.0028	$0.3870^{+0.1843}_{-0.1831}$	
3531 A	2.7694 ± 0.0132	-17.657 ± 0.016	-15.849 ± 0.014	0.124	11.0653 ± 0.0028	$0.8130^{+0.1943}_{-0.2726}$	
3531 B	2.4929 ± 0.4232	-17.963 ± 0.553	-15.183 ± 0.610	1.330	19.8962 ± 0.0117		

TABLE 3 continued

TOI	π [mas]	$\mu_\alpha \cos(\delta)$ [mas/yr]	μ_δ [mas/yr]	$epsi$ [mas]	G [mag]	A_G [mag]	
3533 B	4.1368 ± 0.8172	-3.067 ± 0.773	-13.748 ± 0.805	8.599	12.5867 ± 0.0081		
3533 A	2.3155 ± 0.0105	-7.333 ± 0.010	-13.811 ± 0.011	0.050	12.3977 ± 0.0028	$0.4550^{+0.1468}_{-0.2494}$	
3560 A	3.2964 ± 0.0153	6.494 ± 0.016	1.589 ± 0.019	0.152	11.1630 ± 0.0028	$0.2150^{+0.1330}_{-0.0935}$	
3560 B	3.5079 ± 0.1034	6.785 ± 0.113	0.342 ± 0.137	1.166	14.3548 ± 0.0028		
3584 A	2.2622 ± 0.0278	16.974 ± 0.037	9.218 ± 0.033	0.323	12.9741 ± 0.0028		
3584 B	2.2790 ± 0.0230	17.235 ± 0.048	8.602 ± 0.019	0.098	13.5272 ± 0.0028	$0.0000^{+0.5098}_{-0.0000}$	SHC
3584 C	2.2733 ± 0.0511	17.298 ± 0.063	8.818 ± 0.058	0.000	17.0914 ± 0.0028	$0.3311^{+0.2004}_{-0.2004}$	SHC
3586 A	4.2460 ± 0.0252	-7.353 ± 0.029	15.291 ± 0.029	0.266	12.9751 ± 0.0028	$0.0213^{+0.1764}_{-0.0093}$	
3586 B	4.3772 ± 0.1051	-6.617 ± 0.116	15.471 ± 0.137	0.407	17.9469 ± 0.0035		
3607 A	1.9354 ± 0.0333	8.910 ± 0.050	-11.664 ± 0.041	0.336	14.0234 ± 0.0029		
3607 B	1.8921 ± 0.0368	8.962 ± 0.095	-10.626 ± 0.075	0.209	15.0427 ± 0.0028	$0.0000^{+0.4805}_{-0.0000}$	SHC
3628 A	2.9968 ± 0.0132	37.585 ± 0.014	-12.397 ± 0.011	0.075	12.0879 ± 0.0028	$0.3150^{+0.1870}_{-0.1306}$	
3628 B	2.9882 ± 0.0125	37.716 ± 0.013	-12.074 ± 0.011	0.061	12.2215 ± 0.0028		
3628 C	3.0086 ± 0.1063	37.078 ± 0.089	-14.423 ± 0.338	0.388	16.0404 ± 0.0034		
3634 A	2.0145 ± 0.2116	-8.268 ± 0.203	-4.232 ± 0.122	1.370	12.1373 ± 0.0032		
3634 B	2.4055 ± 0.3678	-6.206 ± 0.418	-4.784 ± 0.160	1.533	12.5085 ± 0.0033		
3636 A	2.2499 ± 0.0166	-9.242 ± 0.015	-16.771 ± 0.016	0.005	13.2711 ± 0.0028	$0.3300^{+0.1700}_{-0.1861}$	
3636 B	5.7508 ± 0.9837	-7.768 ± 0.986	-15.159 ± 0.598	1.432	19.3550 ± 0.0157		
3642 A	2.7064 ± 0.0165	10.396 ± 0.015	-10.158 ± 0.014	0.000	13.0922 ± 0.0028	$0.2423^{+0.1607}_{-0.1641}$	
3642 B	2.4452 ± 0.1005	9.815 ± 0.100	-10.694 ± 0.094	0.302	16.9979 ± 0.0031		
3682 A	2.5213 ± 0.0170	34.818 ± 0.023	-18.553 ± 0.015	0.070	11.8685 ± 0.0028		
3682 B	2.2612 ± 0.0533	35.839 ± 0.068	-13.332 ± 0.044	0.000	15.9081 ± 0.0028	$0.3303^{+0.3697}_{-0.2119}$	
3688 A	2.5118 ± 0.0111	18.777 ± 0.009	-11.398 ± 0.013	0.014	12.3571 ± 0.0028	$0.7613^{+0.2787}_{-0.2634}$	
3688 B	2.5109 ± 0.1834	18.860 ± 0.168	-11.127 ± 0.246	0.549	18.4505 ± 0.0042		
3712 A	2.8275 ± 0.0249	13.023 ± 0.023	-15.880 ± 0.016	0.082	14.1183 ± 0.0028		
3712 B	3.0133 ± 0.1160	13.093 ± 0.106	-15.686 ± 0.077	0.000	17.5023 ± 0.0030	$0.2394^{+0.0189}_{-0.0189}$	SHC
3714 A	8.8385 ± 0.0219	19.826 ± 0.025	-70.762 ± 0.020	0.057	14.2908 ± 0.0028	$0.4560^{+0.4346}_{-0.1474}$	
3714 B	8.8470 ± 0.2265	18.805 ± 0.252	-70.672 ± 0.205	0.190	18.8475 ± 0.0034		
3724 A	2.2760 ± 0.0150	6.687 ± 0.017	-18.321 ± 0.012	0.054	12.1368 ± 0.0028	$0.5900^{+0.1610}_{-0.1327}$	
3724 B	1.6154 ± 0.3318	6.398 ± 0.437	-17.956 ± 0.305	0.871	18.2689 ± 0.0087		
3741 A	2.0778 ± 0.2075	-0.899 ± 0.236	-0.564 ± 0.182	1.673	13.7007 ± 0.0035	$0.5460^{+0.3191}_{-0.3610}$	
3741 B	1.3246 ± 0.0324	-0.592 ± 0.036	-1.069 ± 0.031	0.168	14.6383 ± 0.0041		
3742 B	5.9961 ± 0.0168	40.533 ± 0.021	-29.932 ± 0.018	0.000	13.8193 ± 0.0028	$0.9093^{+0.2657}_{-0.4189}$	
3742 A	5.9830 ± 0.0150	40.490 ± 0.018	-30.866 ± 0.016	0.062	12.9491 ± 0.0028		
3745 A	2.8689 ± 0.0252	6.312 ± 0.025	-19.652 ± 0.017	0.094	13.8210 ± 0.0028		
3745 B	2.8982 ± 0.0271	5.432 ± 0.027	-19.348 ± 0.022	0.107	13.8686 ± 0.0028	$0.6417^{+0.2931}_{-0.3698}$	
3758 A	1.9972 ± 0.0144	0.312 ± 0.011	-6.801 ± 0.014	0.080	13.2349 ± 0.0028	$1.6340^{+0.4285}_{-0.4891}$	
3758 B	1.9234 ± 0.0977	1.280 ± 0.121	-7.528 ± 0.119	0.412	16.5664 ± 0.0034		
3761 B	4.5911 ± 0.0126	17.162 ± 0.008	-26.434 ± 0.012	0.000	13.5745 ± 0.0028		
3761 A	4.6027 ± 0.0098	16.199 ± 0.006	-25.933 ± 0.009	0.041	12.2262 ± 0.0028	$0.2090^{+0.1011}_{-0.0840}$	
3781 A	3.6818 ± 0.0157	-11.557 ± 0.015	-22.175 ± 0.012	0.100	12.9944 ± 0.0028		
3781 B	3.6742 ± 0.0330	-12.882 ± 0.033	-22.261 ± 0.025	0.091	15.6283 ± 0.0028	$0.4810^{+0.5230}_{-0.0961}$	
3791 A	2.0635 ± 0.0089	-4.514 ± 0.011	-14.888 ± 0.013	0.071	11.9164 ± 0.0028		
3791 B	2.0890 ± 0.0091	-4.510 ± 0.011	-14.938 ± 0.012	0.066	12.4252 ± 0.0028	$0.2803^{+0.0887}_{-0.1663}$	
3795 A	2.2947 ± 0.0164	-1.150 ± 0.015	-1.011 ± 0.014	0.090	12.6766 ± 0.0029		
3795 B	2.3590 ± 0.0670	-0.959 ± 0.057	-0.886 ± 0.055	0.212	16.6713 ± 0.0029	$0.0377^{+0.1564}_{-0.0307}$	

TABLE 3 continued

TOI	π [mas]	$\mu_\alpha \cos(\delta)$ [mas/yr]	μ_δ [mas/yr]	$epsi$ [mas]	G [mag]	A_G [mag]	
3797 A	2.4942 ± 0.0148	-7.945 ± 0.015	-6.929 ± 0.013	0.066	12.2200 ± 0.0028		
3797 B	2.4782 ± 0.0263	-8.278 ± 0.028	-7.068 ± 0.025	0.000	14.7839 ± 0.0028	$0.2037^{+0.3781}_{-0.1488}$	
3801 A	2.0122 ± 0.0149	-5.623 ± 0.014	-14.080 ± 0.010	0.000	13.4814 ± 0.0028	$0.6540^{+0.1331}_{-0.2991}$	
3801 B	1.8222 ± 0.2313	-5.501 ± 0.213	-13.954 ± 0.164	0.646	18.7086 ± 0.0070		
3823 A	2.2333 ± 0.0553	-10.275 ± 0.051	-11.383 ± 0.054	0.449	11.8176 ± 0.0028	$0.1570^{+0.1190}_{-0.1481}$	
3823 B	2.6615 ± 0.2345	-9.984 ± 0.213	-10.688 ± 0.201	0.918	18.0512 ± 0.0093		
3828 A	2.8895 ± 0.0136	-11.854 ± 0.012	-36.352 ± 0.014	0.111	11.7578 ± 0.0028	$0.9041^{+0.2465}_{-0.2465}$	SHC
3828 B	2.9390 ± 0.0139	-11.521 ± 0.013	-35.619 ± 0.014	0.114	11.9981 ± 0.0028		
3829 A	2.5534 ± 0.0299	7.929 ± 0.027	-22.846 ± 0.027	0.128	12.8680 ± 0.0028	$0.5270^{+0.2186}_{-0.2884}$	
3829 B	2.2647 ± 0.0746	6.321 ± 0.100	-20.316 ± 0.115	0.229	14.5632 ± 0.0147		
3867 A	2.0764 ± 0.0142	-30.294 ± 0.011	-8.137 ± 0.012	0.088	13.2021 ± 0.0028	$0.4130^{+0.1199}_{-0.2401}$	
3867 B	1.9565 ± 0.2303	-30.050 ± 0.231	-8.052 ± 0.191	1.041	18.9153 ± 0.0062		
3872 A	2.5321 ± 0.0167	12.211 ± 0.015	-27.290 ± 0.014	0.080	12.8266 ± 0.0028		
3872 B	2.5096 ± 0.0565	11.765 ± 0.050	-27.605 ± 0.048	0.423	14.5556 ± 0.0028	$0.2173^{+0.3142}_{-0.2093}$	
3875 A	2.5131 ± 0.0111	6.276 ± 0.014	-23.960 ± 0.013	0.058	12.4824 ± 0.0028		
3875 B	2.3635 ± 0.0392	6.079 ± 0.046	-23.853 ± 0.043	0.377	14.4436 ± 0.0028	$0.8483^{+0.2928}_{-0.4564}$	
3883 A	2.0150 ± 0.0145	-11.230 ± 0.007	-3.464 ± 0.011	0.086	12.2750 ± 0.0028	$0.5400^{+0.2986}_{-0.4084}$	
3883 B	2.0994 ± 0.0864	-11.426 ± 0.040	-3.610 ± 0.061	0.380	17.1427 ± 0.0029		
3889 A	3.2539 ± 0.0139	-28.881 ± 0.013	-36.522 ± 0.016	0.075	12.9323 ± 0.0028		
3889 B	3.2854 ± 0.0295	-27.235 ± 0.027	-35.533 ± 0.033	0.147	15.1588 ± 0.0028	$0.6490^{+0.5260}_{-0.4961}$	
3896 A	5.4600 ± 0.0098	-108.453 ± 0.011	-4.958 ± 0.010	0.055	12.2257 ± 0.0028		
3896 B	5.5026 ± 0.0296	-108.505 ± 0.034	-5.017 ± 0.031	0.091	15.8077 ± 0.0028	$0.3085^{+0.1855}_{-0.1346}$	
3915 A	3.5926 ± 0.0159	-36.921 ± 0.015	35.332 ± 0.011	0.080	12.8996 ± 0.0028	$0.1602^{+0.0479}_{-0.0170}$	
3915 B	3.6064 ± 0.1920	-38.018 ± 0.161	36.095 ± 0.136	0.790	17.3797 ± 0.0062		
3920 A	2.0001 ± 0.0116	10.234 ± 0.012	6.142 ± 0.011	0.000	13.3445 ± 0.0028	$0.9260^{+0.2461}_{-0.3135}$	
3920 B	1.9917 ± 0.0282	10.392 ± 0.031	6.171 ± 0.027	0.127	15.3209 ± 0.0028		
3922 B	3.7843 ± 0.0168	40.170 ± 0.013	-35.715 ± 0.020	0.139	12.7800 ± 0.0028		
3922 A	3.7885 ± 0.0122	39.376 ± 0.010	-35.779 ± 0.014	0.088	12.3127 ± 0.0028	$0.1977^{+0.0914}_{-0.0923}$	
3956 B	2.3213 ± 0.0129	-9.642 ± 0.013	-0.124 ± 0.015	0.039	13.6040 ± 0.0028		
3956 A	2.3444 ± 0.0255	-9.131 ± 0.025	-1.189 ± 0.030	0.258	12.5291 ± 0.0028	$0.5955^{+0.2416}_{-0.1420}$	
3966 A	3.3953 ± 0.2509	-3.736 ± 0.201	-18.230 ± 0.233	2.597	12.6688 ± 0.0034	$0.0347^{+0.1524}_{-0.0248}$	
3966 B	2.8621 ± 0.0911	-3.562 ± 0.071	-19.212 ± 0.086	0.476	17.4805 ± 0.0051		
3977 A	4.4761 ± 0.0093	19.633 ± 0.010	-59.020 ± 0.012	0.057	11.8382 ± 0.0028		
3977 B	4.4895 ± 0.0114	19.414 ± 0.012	-58.492 ± 0.017	0.052	13.1923 ± 0.0028	$0.2340^{+0.3740}_{-0.1737}$	
3984 A	9.1843 ± 0.0191	-48.951 ± 0.016	42.647 ± 0.020	0.056	14.6487 ± 0.0028	$0.2210^{+0.1528}_{-0.1528}$	SHC
3984 B	9.0569 ± 0.2022	-50.379 ± 0.163	40.950 ± 0.212	0.000	19.0813 ± 0.0035		
3998 A	2.4433 ± 0.0109	40.382 ± 0.008	-4.035 ± 0.011	0.025	12.5908 ± 0.0028		
3998 B	2.3977 ± 0.0519	40.274 ± 0.041	-3.563 ± 0.049	0.237	16.4309 ± 0.0036	$0.0000^{+0.2236}_{-0.0000}$	SHC
4001 A	3.1839 ± 0.0099	38.437 ± 0.010	-7.216 ± 0.010	0.036	12.1892 ± 0.0028		
4001 B	3.1813 ± 0.0149	38.834 ± 0.016	-7.364 ± 0.015	0.000	14.0300 ± 0.0028	$0.3650^{+0.1870}_{-0.0320}$	
4021 A	2.0152 ± 0.0150	13.008 ± 0.012	-4.221 ± 0.013	0.124	11.5185 ± 0.0028		
4021 B	2.0244 ± 0.0226	12.367 ± 0.018	-4.988 ± 0.019	0.000	15.1104 ± 0.0028	$0.5990^{+0.2425}_{-0.2863}$	
4040 A	3.3950 ± 0.0120	-0.367 ± 0.015	18.861 ± 0.017	0.084	12.8525 ± 0.0028	$0.0795^{+0.1465}_{-0.0608}$	
4040 B	5.1879 ± 0.9560	-2.278 ± 1.485	14.109 ± 2.231	2.820	20.4319 ± 0.0107		
4059 A	2.9516 ± 0.0118	4.954 ± 0.015	25.093 ± 0.017	0.053	13.6797 ± 0.0028	$0.2560^{+0.1831}_{-0.1080}$	
4059 B	2.7338 ± 0.1000	4.172 ± 0.137	25.217 ± 0.145	0.554	17.8747 ± 0.0032		

TABLE 3 continued

TOI	π [mas]	$\mu_\alpha \cos(\delta)$ [mas/yr]	μ_δ [mas/yr]	ϵ [mas]	G [mag]	A_G [mag]	
4070 B	2.4449 ± 0.0122	8.642 ± 0.013	-18.269 ± 0.016	0.080	13.5274 ± 0.0028		
4070 A	2.6418 ± 0.0200	9.336 ± 0.021	-18.455 ± 0.026	0.230	12.5658 ± 0.0028	0.3410 ^{+0.1836} _{-0.0680}	
4077 A	3.2950 ± 0.0105	14.495 ± 0.010	-5.085 ± 0.014	0.000	13.4583 ± 0.0028	0.2777 ^{+0.1923} _{-0.1073}	
4077 B	3.2764 ± 0.0885	14.505 ± 0.089	-4.694 ± 0.108	0.000	18.0035 ± 0.0030		
4079 B	2.7511 ± 0.0110	17.947 ± 0.008	0.738 ± 0.011	0.041	12.6781 ± 0.0028		
4079 A	2.7324 ± 0.0105	18.083 ± 0.008	0.480 ± 0.011	0.053	11.9719 ± 0.0028	0.6147 ^{+0.1797} _{-0.1797}	SHC
4081 A	2.2178 ± 0.0171	14.352 ± 0.014	-11.890 ± 0.016	0.133	11.1647 ± 0.0028	1.0309 ^{+0.3428} _{-0.3428}	SHC
4081 B	2.2822 ± 0.0283	14.464 ± 0.021	-11.131 ± 0.029	0.165	14.4743 ± 0.0028		
4089 A	2.7202 ± 0.0160	-19.332 ± 0.011	-22.925 ± 0.016	0.140	12.1023 ± 0.0028		
4089 B	2.6560 ± 0.0319	-18.932 ± 0.021	-23.408 ± 0.045	0.171	13.5114 ± 0.0028	0.0000 ^{+0.5071} _{-0.0000}	SHC
4107 A	6.5079 ± 0.0112	-13.776 ± 0.012	6.051 ± 0.014	0.000	13.6674 ± 0.0028	0.2500 ^{+0.3414} _{-0.1203}	
4107 B	6.5573 ± 0.0312	-13.514 ± 0.041	6.105 ± 0.038	0.274	15.0644 ± 0.0028		
4113 A	6.6975 ± 0.0115	12.050 ± 0.016	66.562 ± 0.014	0.089	11.6446 ± 0.0028	0.0163 ^{+0.2653} _{-0.0083}	
4113 B	6.9631 ± 0.0811	12.033 ± 0.121	65.993 ± 0.111	0.316	17.4228 ± 0.0066		
4123 A	4.1430 ± 0.0103	-20.389 ± 0.009	-44.515 ± 0.010	0.040	12.3508 ± 0.0028	0.1300 ^{+0.0777} _{-0.0595}	
4123 B	4.3245 ± 0.1500	-19.309 ± 0.140	-44.204 ± 0.151	0.747	17.9385 ± 0.0072		
4128 A	3.2290 ± 0.0136	-13.190 ± 0.017	-28.915 ± 0.014	0.086	12.7967 ± 0.0028		
4128 B	3.2503 ± 0.0891	-13.814 ± 0.116	-28.874 ± 0.098	0.894	13.7339 ± 0.0028	0.6790 ^{+0.2091} _{-0.1863}	
4145 A	4.9017 ± 0.0096	11.694 ± 0.010	-13.534 ± 0.011	0.041	12.0492 ± 0.0028	0.0890 ^{+0.1631} _{-0.0890}	
4145 B	5.7061 ± 0.1635	11.927 ± 0.199	-16.830 ± 0.588	0.663	17.3670 ± 0.0046		
4168 A	3.0551 ± 0.0147	26.083 ± 0.020	7.243 ± 0.017	0.115	11.8651 ± 0.0028	0.2373 ^{+0.2120} _{-0.1244}	
4168 B	3.1226 ± 0.0175	26.426 ± 0.024	7.408 ± 0.020	0.000	14.5282 ± 0.0028		
4175 A	21.5872 ± 0.0359	140.238 ± 0.038	-140.048 ± 0.027	0.168	8.6339 ± 0.0028		
4175 B	21.8129 ± 0.0399	130.361 ± 0.041	-143.004 ± 0.041	0.168	8.8183 ± 0.0029	0.9002 ^{+0.2040} _{-0.2040}	SHC
4175 C	21.6547 ± 0.0265	135.757 ± 0.031	-139.611 ± 0.018	0.094	13.7833 ± 0.0028	0.0537 ^{+0.2814} _{-0.0403}	
4176 A	2.5915 ± 0.0225	-7.645 ± 0.025	8.934 ± 0.020	0.124	9.7568 ± 0.0028		
4176 B	2.5938 ± 0.0237	-7.619 ± 0.025	8.726 ± 0.022	0.035	14.2051 ± 0.0028	0.1095 ^{+0.1866} _{-0.0216}	
4179 B	10.5358 ± 0.3143	-60.630 ± 0.353	3.599 ± 0.223	2.250	11.0571 ± 0.0030		
4179 A	9.9729 ± 0.0183	-63.043 ± 0.019	9.244 ± 0.014	0.080	9.9922 ± 0.0028	0.0537 ^{+0.1943} _{-0.0367}	
4182 A	7.5383 ± 0.0165	127.765 ± 0.019	58.312 ± 0.020	0.169	9.7074 ± 0.0028		
4182 B	7.5374 ± 0.0391	128.255 ± 0.045	59.187 ± 0.051	0.000	16.5349 ± 0.0029	0.0088 ^{+0.1827} _{-0.0088}	
4192 A	2.0501 ± 0.0120	16.564 ± 0.008	21.665 ± 0.010	0.075	12.2157 ± 0.0028		
4192 B	2.0106 ± 0.0173	16.467 ± 0.011	21.742 ± 0.014	0.035	14.2976 ± 0.0029	0.1340 ^{+0.1190} _{-0.1287}	
4212 A	3.7286 ± 0.3262	-2.836 ± 0.250	4.960 ± 0.322	3.789	12.2259 ± 0.0034	0.5204 ^{+0.2509} _{-0.2509}	SHC
4212 B	7.9975 ± 1.4534	-2.986 ± 0.936	3.312 ± 1.807	11.289	20.3781 ± 0.0128		
4226 A	2.5248 ± 0.4279	-2.122 ± 0.251	-0.653 ± 0.386	3.553	11.6758 ± 0.0028	0.2391 ^{+0.2679} _{-0.2391}	SHC
4226 B	1.9440 ± 0.3435	-2.352 ± 0.262	-1.610 ± 0.284	1.423	19.3122 ± 0.0064		
4245 A	4.7788 ± 0.0124	-17.313 ± 0.014	28.297 ± 0.015	0.106	12.2963 ± 0.0028	0.2000 ^{+0.2976} _{-0.1546}	
4245 B	4.8973 ± 0.1200	-15.771 ± 0.157	28.031 ± 0.130	1.256	15.6363 ± 0.0037		
4293 A	2.1309 ± 0.0145	4.296 ± 0.015	-28.982 ± 0.014	0.000	13.0778 ± 0.0028	0.2693 ^{+0.1750} _{-0.1086}	
4293 B	1.9447 ± 0.1581	3.836 ± 0.147	-28.828 ± 0.148	0.279	18.0305 ± 0.0044		
4301 A	6.9832 ± 0.0111	-64.472 ± 0.009	19.070 ± 0.010	0.049	10.6339 ± 0.0028	0.1005 ^{+0.0936} _{-0.0775}	
4301 B	6.7317 ± 0.2746	-64.162 ± 0.222	19.417 ± 0.351	0	19.0917 ± 0.0037		
4303 A	3.9464 ± 0.0121	45.870 ± 0.013	0.569 ± 0.015	0.104	9.7193 ± 0.0028		
4303 B	3.8848 ± 0.0204	45.560 ± 0.022	0.944 ± 0.025	0.106	14.9661 ± 0.0028	0.3918 ^{+0.3132} _{-0.1708}	
4325 A	19.5256 ± 0.0208	74.703 ± 0.022	-169.873 ± 0.020	0.128	12.9796 ± 0.0028		
4325 B	19.5097 ± 0.0378	74.782 ± 0.040	-170.674 ± 0.036	0.125	15.4419 ± 0.0029	0.2645 ^{+0.1995} _{-0.2515}	
4330 A	3.4820 ± 0.0210	-35.232 ± 0.023	-22.466 ± 0.018	0.089	8.2898 ± 0.0028		
4330 B	3.3770 ± 0.1446	-35.685 ± 0.147	-22.509 ± 0.117	0.958	10.7925 ± 0.0030	0.0000 ^{+0.2837} _{-0.0000}	SHC

TABLE 3 continued

TOI	π [mas]	$\mu_\alpha \cos(\delta)$ [mas/yr]	μ_δ [mas/yr]	ϵ [mas]	G [mag]	A_G [mag]	
4337 B	15.3941 ± 0.0125	-29.822 ± 0.016	0.137 ± 0.014	0.073	12.0277 ± 0.0028		
4337 A	15.4256 ± 0.0136	-29.475 ± 0.017	0.586 ± 0.015	0.083	9.1343 ± 0.0028	$0.1440^{+0.1710}_{-0.0593}$	
4339 B	8.0854 ± 0.0344	-79.059 ± 0.038	23.767 ± 0.034	0.067	15.2500 ± 0.0028		
4339 A	8.1133 ± 0.0203	-78.605 ± 0.022	24.739 ± 0.020	0.000	14.1382 ± 0.0031	$0.2660^{+0.3510}_{-0.1583}$	
4344 A	4.3265 ± 0.0129	8.678 ± 0.019	-20.432 ± 0.017	0.113	9.9133 ± 0.0028		
4344 B	4.2397 ± 0.0716	7.363 ± 0.117	-21.688 ± 0.110	0.604	15.5925 ± 0.0033	$0.0000^{+0.1683}_{-0.0000}$	SHC
4349 A	13.8901 ± 0.0209	278.224 ± 0.019	105.497 ± 0.018	0.144	12.6615 ± 0.0028	$0.6280^{+0.2918}_{-0.2650}$	
4349 B	13.8550 ± 0.1123	280.632 ± 0.098	108.145 ± 0.090	0.825	15.7032 ± 0.0031		
4350 A	9.6729 ± 0.0104	60.757 ± 0.014	32.809 ± 0.013	0.068	9.3749 ± 0.0028	$0.1990^{+0.1670}_{-0.1051}$	
4350 B	9.8182 ± 0.0783	59.892 ± 0.135	32.989 ± 0.105	0.557	16.2487 ± 0.0067		
4359 A	5.6784 ± 0.0133	-31.415 ± 0.014	7.856 ± 0.013	0.064	9.8537 ± 0.0028		
4359 B	5.6001 ± 0.0350	-32.032 ± 0.037	8.286 ± 0.038	0.000	15.8062 ± 0.0028	$0.3085^{+0.1581}_{-0.1346}$	
4366 A	3.9742 ± 0.0114	3.884 ± 0.011	8.440 ± 0.013	0.056	10.6782 ± 0.0028	$1.7163^{+0.3779}_{-0.4574}$	
4366 B	3.9719 ± 0.0250	4.460 ± 0.025	8.453 ± 0.031	0.000	15.4737 ± 0.0028		
4369 A	3.5212 ± 0.0707	19.215 ± 0.086	-30.255 ± 0.103	0.898	9.6646 ± 0.0028		
4369 B	3.9721 ± 0.0108	19.750 ± 0.013	-29.086 ± 0.015	0.094	10.0921 ± 0.0028	$0.1577^{+0.1633}_{-0.1577}$	SHC
4370 A	4.6221 ± 0.0228	10.196 ± 0.024	-17.865 ± 0.017	0.126	9.7265 ± 0.0028		
4370 B	4.6662 ± 0.0737	9.120 ± 0.084	-17.807 ± 0.052	0.123	16.7804 ± 0.0029	$0.0470^{+0.0485}_{-0.0200}$	
4372 A	5.5395 ± 0.0924	-34.738 ± 0.096	-1.817 ± 0.111	1.076	10.9396 ± 0.0029	$0.4855^{+0.2555}_{-0.1292}$	
4372 B	4.4002 ± 0.2861	-35.293 ± 0.365	0.883 ± 0.347	0.764	19.0876 ± 0.0056		
4390 A	5.2425 ± 0.0297	2.629 ± 0.032	-16.757 ± 0.023	0.184	9.9879 ± 0.0028	$1.0367^{+0.1785}_{-0.1785}$	SHC
4390 B	5.2339 ± 0.0345	4.544 ± 0.048	-16.374 ± 0.043	0.177	10.7970 ± 0.0031		
4414 B	3.0877 ± 0.0483	7.006 ± 0.119	-9.873 ± 0.093	0.182	10.9572 ± 0.0048		
4414 A	2.9238 ± 0.0388	7.477 ± 0.047	-11.069 ± 0.027	0.223	9.7974 ± 0.0028		
4420 A	4.3436 ± 0.0153	4.434 ± 0.011	13.946 ± 0.015	0.120	9.9512 ± 0.0028		
4420 B	4.3890 ± 0.0238	4.405 ± 0.021	14.824 ± 0.021	0.195	13.1066 ± 0.0028	$0.6837^{+0.1444}_{-0.1797}$	
4425 A	5.6925 ± 0.0172	1.971 ± 0.019	-19.267 ± 0.013	0.019	9.7596 ± 0.0028	$0.4535^{+0.2353}_{-0.2038}$	
4425 B	5.6703 ± 0.0514	1.793 ± 0.054	-19.380 ± 0.040	0.252	15.4223 ± 0.0031		
4463 A	5.6588 ± 0.0175	-5.157 ± 0.017	50.619 ± 0.017	0.114	10.9509 ± 0.0028		
4463 B	5.6443 ± 0.0673	-5.258 ± 0.068	50.977 ± 0.072	0.154	16.7682 ± 0.0028	$0.2078^{+0.2088}_{-0.1911}$	
4499 A	5.6756 ± 0.0112	22.425 ± 0.012	29.132 ± 0.012	0.083	10.5265 ± 0.0028	$0.1210^{+0.0916}_{-0.0758}$	
4499 B	5.6949 ± 0.0712	22.160 ± 0.080	28.727 ± 0.085	0.000	17.6678 ± 0.0030		
4522 A	4.4347 ± 0.0820	-44.513 ± 0.122	-32.865 ± 0.058	0.039	16.8183 ± 0.0029	$0.3520^{+0.0934}_{-0.0951}$	
4522 B	4.6178 ± 0.1908	-43.880 ± 0.270	-32.646 ± 0.135	0.000	18.4140 ± 0.0032		
4546 B	3.0908 ± 0.0189	-12.745 ± 0.019	-4.971 ± 0.016	0.081	10.3908 ± 0.0028		
4546 A	3.0928 ± 0.0179	-12.969 ± 0.019	-4.561 ± 0.017	0.087	10.2763 ± 0.0028	$0.5792^{+0.2598}_{-0.2598}$	SHC

TABLE 3 continued

CTOI	π [mas]	$\mu_\alpha \cos(\delta)$ [mas/yr]	μ_δ [mas/yr]	$epsi$ [mas]	G [mag]	A_G [mag]	
13073396 A	13.6999 ± 0.0201	233.697 ± 0.019	-43.183 ± 0.021	0.000	14.2910 ± 0.0028	$0.3730^{+0.0630}_{-0.0795}$	
13073396 B	13.7098 ± 0.0707	233.767 ± 0.068	-43.338 ± 0.076	0.208	16.9415 ± 0.0029		
37652870 A	8.5465 ± 0.0199	37.417 ± 0.028	-95.894 ± 0.015	0.111	11.8993 ± 0.0028	$0.2420^{+0.1480}_{-0.2180}$	
37652870 B	8.5967 ± 0.0641	37.070 ± 0.093	-95.310 ± 0.047	0.000	16.5463 ± 0.0029		
94984950 A	6.4511 ± 0.0353	-19.187 ± 0.045	-17.146 ± 0.036	0.239	8.5150 ± 0.0028	$0.4095^{+0.2060}_{-0.2225}$	
94984950 B	6.2177 ± 0.3024	-19.341 ± 0.362	-16.500 ± 0.294	1.448	18.8199 ± 0.0046		
145601161 A	7.6210 ± 0.0164	-33.385 ± 0.019	19.478 ± 0.019	0.117	7.8660 ± 0.0028		
145601161 B	7.5985 ± 0.0239	-34.139 ± 0.027	19.929 ± 0.027	0.000	15.4224 ± 0.0028	$0.5163^{+0.5638}_{-0.3434}$	
219018744 A	2.7303 ± 0.0118	-19.052 ± 0.014	2.823 ± 0.014	0.118	11.2881 ± 0.0028		
219018744 B	2.7549 ± 0.0165	-18.928 ± 0.019	2.574 ± 0.019	0.057	14.6660 ± 0.0028	$1.2060^{+0.3447}_{-0.3380}$	
228463329 A	18.3964 ± 0.0171	-39.288 ± 0.022	-139.784 ± 0.015	0.088	9.0851 ± 0.0028		
228463329 B	18.0229 ± 0.0405	-34.876 ± 0.049	-142.324 ± 0.038	0.235	14.8987 ± 0.0028	$0.2842^{+0.3738}_{-0.0872}$	
248960573 A	4.8017 ± 0.0329	20.737 ± 0.036	-10.531 ± 0.015	0.219	11.9581 ± 0.0028		
248960573 B	4.5996 ± 0.0466	18.458 ± 0.061	-11.062 ± 0.018	0.234	12.7345 ± 0.0029		
323717669 A	2.1779 ± 0.0446	6.139 ± 0.048	-1.741 ± 0.041	0.349	15.6208 ± 0.0031		
323717669 B	2.0469 ± 0.0915	5.543 ± 0.119	-2.040 ± 0.076	0.330	17.4829 ± 0.0033	$0.0000^{+0.0405}_{-0.0000}$	SHC
333785427 A	2.5728 ± 0.0159	18.637 ± 0.022	16.588 ± 0.017	0.098	10.5174 ± 0.0028		
333785427 B	2.4686 ± 0.0533	19.464 ± 0.096	17.080 ± 0.060	0.372	14.3363 ± 0.0035	$0.0000^{+0.4962}_{-0.0000}$	SHC
345327044 A	4.8734 ± 0.0124	-5.968 ± 0.011	-1.929 ± 0.012	0.070	9.7515 ± 0.0028		
345327044 B	4.8611 ± 0.0534	-5.899 ± 0.051	-2.238 ± 0.047	0.000	16.8535 ± 0.0028	$0.1682^{+0.0769}_{-0.1473}$	

TABLE 4 This table lists for each detected companion (sorted by its identifier) the angular separation ρ and position angle PA to the associated (C)TOI, the difference between its parallax and that of the (C)TOI $\Delta\pi$ with its significance (in brackets calculated also by taking into account the Gaia astrometric excess noise), the differential proper motion μ_{rel} of the companion relative to the (C)TOI with its significance, as well as its *cpm-index*. The last column indicates (★) if the detected companion is not listed in the WDS as companion(-candidate) of the (C)TOI.

TOI	ρ [arcsec]	PA [°]	$\Delta\pi$ [mas]	<i>sig-</i> $\Delta\pi$	μ_{rel} [mas/yr]	<i>sig-</i> μ_{rel}	<i>cpm-</i> <i>index</i>	not in WDS
2689 B	7.17645 ± 0.00003	198.47578 ± 0.00023	0.05 ± 0.04	1.1 (1.1)	0.13 ± 0.05	2.9	438	★
2690 A	25.66048 ± 0.00002	223.43721 ± 0.00004	0.05 ± 0.03	1.8 (0.3)	0.44 ± 0.03	16.9	61	
2690 C	1.88688 ± 0.00002	101.16665 ± 0.00084	0.17 ± 0.04	4.8 (0.8)	0.86 ± 0.04	22.0	31	
2690 D	24.62012 ± 0.00004	228.07745 ± 0.00009	0.05 ± 0.05	0.9 (0.1)	2.41 ± 0.06	43.4	12	★
2713 B	3.24708 ± 0.00004	350.21217 ± 0.00065	0.01 ± 0.05	0.1 (0.1)	0.69 ± 0.05	15.3	62	★
2774 B	8.56139 ± 0.00008	169.14922 ± 0.00054	0.02 ± 0.12	0.2 (0.0)	1.07 ± 0.10	10.9	15	★
2803 B	19.53826 ± 0.00001	36.35171 ± 0.00003	0.00 ± 0.02	0.0 (0.0)	0.08 ± 0.01	5.4	304	
2816 A	9.53407 ± 0.00001	170.70583 ± 0.00008	0.04 ± 0.02	2.2 (0.6)	0.49 ± 0.02	27.8	77	★
2892 B	2.95539 ± 0.00004	357.17196 ± 0.00081	0.10 ± 0.04	2.2 (0.2)	0.94 ± 0.06	15.5	22	★
2909 B	2.70811 ± 0.00008	264.98418 ± 0.00211	0.48 ± 0.12	4.0 (0.4)	0.40 ± 0.13	3.1	54	★
2911 B	2.26739 ± 0.00004	66.80964 ± 0.00118	0.05 ± 0.05	1.1 (0.1)	0.23 ± 0.05	4.4	451	★
2956 B	19.44621 ± 0.00009	34.36312 ± 0.00026	0.11 ± 0.10	1.1 (0.6)	0.30 ± 0.12	2.5	104	★
3039 B	21.63875 ± 0.00027	142.41055 ± 0.00068	0.19 ± 0.29	0.7 (0.2)	3.72 ± 0.35	10.8	13	★
3040 B	3.45514 ± 0.00001	301.42787 ± 0.00020	0.01 ± 0.01	1.0 (0.2)	0.17 ± 0.02	10.9	397	
3073 B	0.82393 ± 0.00006	266.49870 ± 0.00874	0.23 ± 0.12	2.0 (0.3)	6.98 ± 0.11	65.3	27	★
3097 B	1.38787 ± 0.00003	146.25381 ± 0.00104	0.01 ± 0.04	0.2 (0.1)	0.39 ± 0.04	10.1	158	★
3106 B	7.33242 ± 0.00012	50.91045 ± 0.00087	0.30 ± 0.15	2.0 (0.7)	7.69 ± 0.17	45.7	10	★
3106 C	2.28695 ± 0.00024	12.33189 ± 0.00517	0.11 ± 0.28	0.4 (0.2)	0.64 ± 0.35	1.8	111	★
3106 D	8.89263 ± 0.00026	49.51842 ± 0.00163	0.12 ± 0.33	0.4 (0.2)	7.91 ± 0.36	22.1	10	★
3155 B	33.36339 ± 0.00004	122.33834 ± 0.00007	0.02 ± 0.06	0.2 (0.2)	0.13 ± 0.05	2.6	449	★
3159 B	4.18948 ± 0.00004	351.10910 ± 0.00062	0.05 ± 0.06	0.8 (0.2)	0.07 ± 0.05	1.2	486	★
3179 B	1.02289 ± 0.00005	358.32287 ± 0.00344	0.02 ± 0.07	0.2 (0.1)	1.27 ± 0.11	11.9	33	★
3202 B	6.55316 ± 0.00011	223.68858 ± 0.00099	0.14 ± 0.15	1.0 (0.6)	0.20 ± 0.16	1.2	211	★
3205 B	2.02292 ± 0.00007	179.66562 ± 0.00238	0.05 ± 0.09	0.6 (0.1)	1.40 ± 0.10	14.1	194	★
3250 B	2.14908 ± 0.00011	327.62262 ± 0.00280	0.11 ± 0.15	0.7 (0.2)	0.58 ± 0.15	4.0	98	★
3252 B	14.15443 ± 0.00002	204.11227 ± 0.00009	0.02 ± 0.03	0.7 (0.2)	0.09 ± 0.03	3.2	1473	
3266 B	1.10865 ± 0.00004	331.04209 ± 0.00204	0.03 ± 0.03	1.0 (0.1)	0.47 ± 0.05	9.6	60	★
3277 B	2.27516 ± 0.00005	337.83142 ± 0.00114	0.08 ± 0.07	1.2 (0.2)	0.24 ± 0.05	4.7	1031	★
3284 B	3.99765 ± 0.00021	309.41286 ± 0.00303	0.17 ± 0.26	0.7 (0.2)	0.13 ± 0.26	0.5	64	★
3288 B	2.16795 ± 0.00008	24.08708 ± 0.00228	0.42 ± 0.12	3.4 (0.9)	0.89 ± 0.08	11.7	49	★
3294 B	1.89610 ± 0.00002	133.59492 ± 0.00055	0.11 ± 0.03	3.7 (0.6)	0.99 ± 0.02	48.2	21	★
3314 B	2.27769 ± 0.00009	199.87840 ± 0.00238	0.22 ± 0.10	2.2 (0.6)	1.08 ± 0.11	10.2	14	★
3342 A	22.32103 ± 0.00002	91.13391 ± 0.00005	0.07 ± 0.03	2.3 (0.4)	0.08 ± 0.02	3.4	687	★
3344 B	2.19552 ± 0.00004	331.34953 ± 0.00105	0.04 ± 0.06	0.8 (0.3)	0.95 ± 0.05	17.6	21	★
3353 B	102.62278 ± 0.00003	100.37374 ± 0.00002	0.01 ± 0.03	0.2 (0.0)	2.67 ± 0.04	63.4	30	★
3355 B	2.33226 ± 0.00010	318.04192 ± 0.00245	0.32 ± 0.10	3.2 (0.7)	0.33 ± 0.13	2.5	238	★
3386 B	4.46341 ± 0.00027	201.05920 ± 0.00311	0.47 ± 0.31	1.5 (0.7)	0.37 ± 0.29	1.3	21	★
3398 B	6.02272 ± 0.00017	136.22144 ± 0.00164	0.19 ± 0.21	0.9 (0.3)	1.18 ± 0.16	7.5	122	★
3444 B	3.17404 ± 0.00031	181.89753 ± 0.00812	0.07 ± 0.54	0.1 (0.1)	1.88 ± 0.56	3.3	12	★
3450 B	0.88187 ± 0.00006	248.86655 ± 0.00454	0.50 ± 0.08	6.0 (0.8)	1.28 ± 0.10	12.8	37	★
3490 A	7.60632 ± 0.00001	321.25483 ± 0.00010	0.01 ± 0.01	0.5 (0.1)	1.01 ± 0.02	58.4	46	★
3491 B	15.15459 ± 0.00013	71.90827 ± 0.00035	0.14 ± 0.15	0.9 (0.1)	0.84 ± 0.19	4.4	39	★
3492 B	46.69394 ± 0.00131	297.58032 ± 0.00165	0.88 ± 1.22	0.7 (0.3)	0.19 ± 1.56	0.1	93	★

TABLE 4 continued

TOI	ρ [arcsec]	PA [$^{\circ}$]	$\Delta\pi$ [mas]	sig - $\Delta\pi$	μ_{rel} [mas/yr]	sig - μ_{rel}	cpm - $index$	not in WDS
3500 B	3.73911 ± 0.00002	34.58936 ± 0.00043	0.02 ± 0.04	0.4 (0.1)	2.14 ± 0.04	54.5	65	★
3503 A	5.71345 ± 0.00002	149.90553 ± 0.00026	0.04 ± 0.03	1.3 (0.1)	0.92 ± 0.04	26.1	32	
3504 A	17.69730 ± 0.00001	260.57265 ± 0.00004	0.03 ± 0.02	1.8 (0.3)	0.11 ± 0.01	7.3	212	
3514 B	1.75837 ± 0.00004	106.70558 ± 0.00180	0.01 ± 0.06	0.2 (0.0)	0.65 ± 0.07	10.1	45	★
3522 B	3.74943 ± 0.00001	220.37650 ± 0.00021	0.02 ± 0.02	0.9 (0.9)	0.19 ± 0.02	10.4	83	★
3531 B	5.35685 ± 0.00035	280.59376 ± 0.00490	0.28 ± 0.42	0.7 (0.2)	0.73 ± 0.60	1.2	64	★
3533 A	2.53039 ± 0.00056	283.10339 ± 0.01415	1.82 ± 0.82	2.2 (0.2)	4.27 ± 0.77	5.5	6.9	★
3560 B	32.09228 ± 0.00009	215.70110 ± 0.00016	0.21 ± 0.10	2.0 (0.2)	1.28 ± 0.14	9.3	10	★
3584 B	1.09294 ± 0.00003	349.04279 ± 0.00229	0.02 ± 0.04	0.5 (0.0)	0.67 ± 0.04	15.8	58	★
3584 C	10.42956 ± 0.00005	11.69081 ± 0.00029	0.01 ± 0.06	0.2 (0.0)	0.51 ± 0.07	7.4	75	★
3586 B	26.01437 ± 0.00010	50.04982 ± 0.00022	0.13 ± 0.11	1.2 (0.3)	0.76 ± 0.12	6.3	45	★
3607 B	0.86206 ± 0.00006	36.18836 ± 0.00398	0.04 ± 0.05	0.9 (0.1)	1.04 ± 0.09	12.2	27	★
3628 B	22.34937 ± 0.00001	214.12449 ± 0.00004	0.01 ± 0.02	0.5 (0.1)	0.35 ± 0.02	21.6	227	
3628 C	21.69589 ± 0.00033	211.11492 ± 0.00057	0.01 ± 0.11	0.1 (0.0)	2.09 ± 0.33	6.4	38	★
3634 B	0.36604 ± 0.00024	167.70988 ± 0.08003	0.39 ± 0.42	0.9 (0.2)	2.13 ± 0.45	4.7	8.0	★
3636 B	2.97490 ± 0.00087	294.86060 ± 0.01023	3.50 ± 0.98	3.6 (2.0)	2.18 ± 0.80	2.7	17	★
3642 B	2.03556 ± 0.00007	170.81970 ± 0.00243	0.26 ± 0.10	2.6 (0.8)	0.79 ± 0.10	8.0	37	★
3682 B	21.81466 ± 0.00004	334.66086 ± 0.00013	0.26 ± 0.06	4.6 (2.9)	5.32 ± 0.05	111.6	15	★
3688 B	4.96403 ± 0.00016	336.69639 ± 0.00144	0.00 ± 0.18	0.0 (0.0)	0.28 ± 0.24	1.2	155	★
3712 B	25.97798 ± 0.00009	325.50149 ± 0.00020	0.19 ± 0.12	1.6 (1.3)	0.21 ± 0.08	2.5	199	★
3714 B	2.66971 ± 0.00019	106.41590 ± 0.00263	0.01 ± 0.23	0.0 (0.0)	1.02 ± 0.25	4.1	143	★
3724 B	1.72747 ± 0.00024	247.92145 ± 0.00673	0.66 ± 0.33	2.0 (0.7)	0.47 ± 0.36	1.3	83	★
3741 B	1.69562 ± 0.00016	263.30954 ± 0.00438	0.75 ± 0.21	3.6 (0.4)	0.59 ± 0.20	2.9	3.7	★
3742 A	3.70115 ± 0.00002	358.27300 ± 0.00029	0.01 ± 0.02	0.6 (0.2)	0.93 ± 0.02	38.8	108	★
3745 B	1.84484 ± 0.00003	79.16503 ± 0.00068	0.03 ± 0.04	0.8 (0.2)	0.93 ± 0.04	25.9	44	★
3758 B	1.24652 ± 0.00008	204.94901 ± 0.00362	0.07 ± 0.10	0.7 (0.2)	1.21 ± 0.12	10.0	12	★
3761 A	4.99206 ± 0.00001	12.41282 ± 0.00010	0.01 ± 0.02	0.7 (0.3)	1.09 ± 0.01	96.5	57	★
3781 B	12.68772 ± 0.00003	151.58995 ± 0.00013	0.01 ± 0.04	0.2 (0.1)	1.33 ± 0.04	36.7	38	★
3791 B	9.68258 ± 0.00001	187.37463 ± 0.00007	0.03 ± 0.01	2.0 (0.3)	0.05 ± 0.02	2.8	621	
3795 B	8.57354 ± 0.00005	201.24130 ± 0.00036	0.06 ± 0.07	0.9 (0.3)	0.23 ± 0.06	3.9	12	★
3797 B	8.88802 ± 0.00003	35.96399 ± 0.00016	0.02 ± 0.03	0.5 (0.2)	0.36 ± 0.03	11.5	59	★
3801 B	2.93556 ± 0.00015	359.74432 ± 0.00342	0.19 ± 0.23	0.8 (0.3)	0.18 ± 0.19	0.9	172	★
3823 B	3.32667 ± 0.00017	264.78039 ± 0.00325	0.43 ± 0.24	1.8 (0.4)	0.75 ± 0.21	3.6	40	★
3828 B	1.44861 ± 0.00001	328.16529 ± 0.00055	0.05 ± 0.02	2.5 (0.3)	0.81 ± 0.02	41.4	94	★
3829 B	1.47567 ± 0.00007	56.87083 ± 0.00261	0.29 ± 0.08	3.6 (1.1)	3.00 ± 0.11	26.3	15	★
3867 B	2.73594 ± 0.00015	190.79063 ± 0.00362	0.12 ± 0.23	0.5 (0.1)	0.26 ± 0.23	1.1	242	★
3872 B	2.37493 ± 0.00005	245.35337 ± 0.00108	0.02 ± 0.06	0.4 (0.1)	0.55 ± 0.05	10.6	110	★
3875 B	18.14488 ± 0.00004	22.79862 ± 0.00012	0.15 ± 0.04	3.7 (0.4)	0.22 ± 0.05	4.7	220	★
3883 B	5.24150 ± 0.00004	81.33593 ± 0.00062	0.08 ± 0.09	1.0 (0.2)	0.24 ± 0.05	5.0	97	★
3889 B	2.27171 ± 0.00002	265.57761 ± 0.00062	0.03 ± 0.03	1.0 (0.2)	1.92 ± 0.03	60.2	48	★
3896 B	17.87801 ± 0.00003	122.79499 ± 0.00008	0.04 ± 0.03	1.4 (0.4)	0.08 ± 0.03	2.3	2762	
3915 B	1.70971 ± 0.00016	268.19507 ± 0.00396	0.01 ± 0.19	0.1 (0.0)	1.34 ± 0.15	8.7	77	★
3920 B	1.68308 ± 0.00002	190.40474 ± 0.00091	0.01 ± 0.03	0.3 (0.1)	0.16 ± 0.03	4.9	150	★
3922 A	2.08039 ± 0.00002	225.86255 ± 0.00045	0.00 ± 0.02	0.2 (0.0)	0.80 ± 0.02	48.4	134	★
3956 A	4.08617 ± 0.00002	265.86837 ± 0.00036	0.02 ± 0.03	0.8 (0.1)	1.18 ± 0.03	36.2	16	★
3966 B	2.81173 ± 0.00019	56.91994 ± 0.00398	0.53 ± 0.27	2.0 (0.2)	1.00 ± 0.25	4.0	38	★
3977 B	2.95021 ± 0.00001	46.82758 ± 0.00025	0.01 ± 0.01	0.9 (0.2)	0.57 ± 0.02	28.4	217	★

TABLE 4 continued

TOI	ρ [arcsec]	PA [°]	$\Delta\pi$ [mas]	sig - $\Delta\pi$	μ_{rel} [mas/yr]	sig - μ_{rel}	cpm - $index$	not in WDS
3984 B	3.27064 ± 0.00015	343.07874 ± 0.00231	0.13 ± 0.20	0.6 (0.6)	2.22 ± 0.19	11.4	59	★
3998 B	2.16139 ± 0.00003	54.20794 ± 0.00096	0.05 ± 0.05	0.9 (0.2)	0.48 ± 0.05	9.7	167	★
4001 B	10.33196 ± 0.00001	307.08633 ± 0.00008	0.00 ± 0.02	0.1 (0.1)	0.42 ± 0.02	22.6	186	★
4021 B	11.36437 ± 0.00002	251.72711 ± 0.00009	0.01 ± 0.03	0.3 (0.1)	1.00 ± 0.02	44.5	27	★
4040 B	3.35613 ± 0.00120	8.87701 ± 0.01400	1.79 ± 0.96	1.9 (0.6)	5.12 ± 2.14	2.4	6.5	★
4059 B	3.53855 ± 0.00010	218.08460 ± 0.00156	0.22 ± 0.10	2.2 (0.4)	0.79 ± 0.14	5.7	65	★
4070 A	3.74492 ± 0.00002	27.88078 ± 0.00032	0.20 ± 0.02	8.4 (0.8)	0.72 ± 0.03	28.6	57	★
4077 B	15.58884 ± 0.00008	37.90108 ± 0.00028	0.02 ± 0.09	0.2 (0.2)	0.39 ± 0.11	3.6	78	★
4079 A	11.46628 ± 0.00001	225.03099 ± 0.00005	0.02 ± 0.02	1.2 (0.3)	0.29 ± 0.01	19.8	124	★
4081 B	2.17240 ± 0.00002	257.98470 ± 0.00063	0.06 ± 0.03	1.9 (0.3)	0.77 ± 0.03	23.3	48	★
4089 B	1.15891 ± 0.00002	58.38509 ± 0.00123	0.06 ± 0.04	1.8 (0.3)	0.63 ± 0.04	15.8	96	★
4107 B	12.35119 ± 0.00004	117.98406 ± 0.00016	0.05 ± 0.03	1.5 (0.2)	0.27 ± 0.04	6.3	112	★
4113 B	3.55473 ± 0.00008	74.02587 ± 0.00142	0.27 ± 0.08	3.2 (0.8)	0.57 ± 0.11	5.1	237	★
4123 B	2.56674 ± 0.00012	359.63176 ± 0.00228	0.18 ± 0.15	1.2 (0.2)	1.12 ± 0.14	8.0	86	★
4128 B	23.74700 ± 0.00007	328.63903 ± 0.00018	0.02 ± 0.09	0.2 (0.0)	0.63 ± 0.12	5.3	102	
4145 B	1.74266 ± 0.00040	41.46992 ± 0.01178	0.80 ± 0.16	4.9 (1.2)	3.30 ± 0.59	5.6	12	★
4168 B	8.56570 ± 0.00002	293.72152 ± 0.00013	0.07 ± 0.02	3.0 (0.6)	0.38 ± 0.03	12.5	143	★
4175 B	1.61034 ± 0.00004	259.76981 ± 0.00139	0.23 ± 0.05	4.2 (0.9)	10.31 ± 0.06	186.2	38	
4175 C	166.81119 ± 0.00003	178.24945 ± 0.00001	0.07 ± 0.04	1.5 (0.3)	4.50 ± 0.05	92.1	87	
4176 B	24.27219 ± 0.00002	335.40461 ± 0.00006	0.00 ± 0.03	0.1 (0.0)	0.21 ± 0.03	7.0	111	★
4179 A	38.08353 ± 0.00019	165.02820 ± 0.00037	0.56 ± 0.31	1.8 (0.2)	6.14 ± 0.25	24.8	20	
4182 B	17.45414 ± 0.00004	330.08316 ± 0.00013	0.00 ± 0.04	0.0 (0.0)	1.00 ± 0.05	18.8	281	★
4192 B	2.73019 ± 0.00001	288.26841 ± 0.00030	0.04 ± 0.02	1.9 (0.5)	0.12 ± 0.02	8.2	440	★
4212 B	26.92283 ± 0.00119	184.80178 ± 0.00154	4.27 ± 1.49	2.9 (0.4)	1.65 ± 1.83	0.9	6.1	★
4226 B	5.62051 ± 0.00038	15.78624 ± 0.00280	0.58 ± 0.55	1.1 (0.2)	0.98 ± 0.47	2.1	5.1	★
4245 B	1.65324 ± 0.00011	157.97771 ± 0.00392	0.12 ± 0.12	1.0 (0.1)	1.56 ± 0.16	10.0	42	★
4293 B	2.49352 ± 0.00008	332.65097 ± 0.00234	0.19 ± 0.16	1.2 (0.6)	0.49 ± 0.15	3.3	120	★
4301 B	34.80516 ± 0.00022	104.73358 ± 0.00052	0.25 ± 0.28	0.9 (0.9)	0.47 ± 0.30	1.5	288	★
4303 B	9.11370 ± 0.00002	158.50453 ± 0.00013	0.06 ± 0.02	2.6 (0.4)	0.49 ± 0.03	17.5	188	★
4325 B	25.29992 ± 0.00003	356.26082 ± 0.00008	0.02 ± 0.04	0.4 (0.1)	0.80 ± 0.04	19.5	462	
4330 B	2.18530 ± 0.00010	3.90890 ± 0.00363	0.11 ± 0.15	0.7 (0.1)	0.46 ± 0.15	3.1	185	
4337 A	5.10545 ± 0.00002	209.01323 ± 0.00019	0.03 ± 0.02	1.7 (0.3)	0.57 ± 0.02	26.2	105	
4339 A	3.62569 ± 0.00003	162.07409 ± 0.00053	0.03 ± 0.04	0.7 (0.4)	1.07 ± 0.04	26.6	154	★
4344 B	2.10247 ± 0.00007	248.43131 ± 0.00236	0.09 ± 0.07	1.2 (0.1)	1.82 ± 0.12	15.8	25	★
4349 B	2.68110 ± 0.00008	12.35082 ± 0.00193	0.04 ± 0.11	0.3 (0.0)	3.58 ± 0.10	37.5	167	★
4350 B	3.80322 ± 0.00007	359.59813 ± 0.00138	0.15 ± 0.08	1.8 (0.3)	0.88 ± 0.13	6.6	156	★
4359 B	15.49053 ± 0.00003	129.51739 ± 0.00012	0.08 ± 0.04	2.1 (1.1)	0.75 ± 0.04	18.9	87	★
4366 B	19.35358 ± 0.00002	325.19177 ± 0.00007	0.00 ± 0.03	0.1 (0.0)	0.58 ± 0.03	21.1	33	★
4369 B	6.11232 ± 0.00007	354.48099 ± 0.00067	0.45 ± 0.07	6.3 (0.5)	1.29 ± 0.10	12.7	55	
4370 B	30.52375 ± 0.00007	75.16433 ± 0.00010	0.04 ± 0.08	0.6 (0.2)	1.08 ± 0.09	12.3	38	★
4372 B	3.48683 ± 0.00025	249.86993 ± 0.00413	1.14 ± 0.30	3.8 (0.8)	2.76 ± 0.36	7.6	25	★
4390 B	1.11151 ± 0.00005	53.91390 ± 0.00252	0.01 ± 0.05	0.2 (0.0)	1.95 ± 0.06	34.0	17	
4414 A	0.89987 ± 0.00014	314.71208 ± 0.00859	0.16 ± 0.06	2.6 (0.6)	1.29 ± 0.10	12.7	20	
4420 B	4.61200 ± 0.00002	14.30015 ± 0.00024	0.05 ± 0.03	1.6 (0.2)	0.88 ± 0.03	34.0	34	
4425 B	5.00122 ± 0.00004	205.10110 ± 0.00050	0.02 ± 0.05	0.4 (0.1)	0.21 ± 0.05	4.0	184	★
4463 B	11.36997 ± 0.00004	107.62112 ± 0.00025	0.01 ± 0.07	0.2 (0.1)	0.37 ± 0.07	5.0	275	★
4499 B	14.56409 ± 0.00007	187.77535 ± 0.00023	0.02 ± 0.07	0.3 (0.2)	0.48 ± 0.08	5.7	151	★
4522 B	7.04849 ± 0.00018	270.63678 ± 0.00111	0.18 ± 0.21	0.9 (0.9)	0.67 ± 0.28	2.4	164	★
4546 A	7.66036 ± 0.00002	207.34741 ± 0.00016	0.00 ± 0.03	0.1 (0.0)	0.47 ± 0.02	19.3	59	★

TABLE 4 continued

CTOI	ρ [arcsec]	PA [°]	$\Delta\pi$ [mas]	sig - $\Delta\pi$	μ_{rel} [mas/yr]	sig - μ_{rel}	cpm - $index$	not in WDS
13073396 B	67.96994 ± 0.00007	214.30476 ± 0.00006	0.01 ± 0.07	0.1 (0.0)	0.17 ± 0.08	2.2	2795	
37652870 B	46.09297 ± 0.00006	290.98867 ± 0.00006	0.05 ± 0.07	0.7 (0.4)	0.68 ± 0.07	10.4	302	
94984950 B	14.27266 ± 0.00028	71.24118 ± 0.00078	0.23 ± 0.30	0.8 (0.2)	0.66 ± 0.30	2.2	77	★
145601161 B	21.98785 ± 0.00002	281.75747 ± 0.00007	0.02 ± 0.03	0.8 (0.2)	0.88 ± 0.03	26.6	89	★
219018744 B	13.34805 ± 0.00002	243.02983 ± 0.00008	0.02 ± 0.02	1.2 (0.2)	0.28 ± 0.02	11.8	138	★
228463329 B	21.27769 ± 0.00004	256.02820 ± 0.00010	0.37 ± 0.04	8.5 (1.5)	5.09 ± 0.05	100.2	57	★
248960573 B	0.83697 ± 0.00002	0.35273 ± 0.00358	0.20 ± 0.06	3.5 (0.6)	2.34 ± 0.07	33.8	19	★
323717669 B	1.19821 ± 0.00007	357.12315 ± 0.00532	0.13 ± 0.10	1.3 (0.3)	0.67 ± 0.12	5.5	18	★
333785427 B	1.41681 ± 0.00005	21.19582 ± 0.00259	0.10 ± 0.06	1.9 (0.3)	0.96 ± 0.09	10.6	53	★
345327044 B	27.39360 ± 0.00004	222.34293 ± 0.00008	0.01 ± 0.05	0.2 (0.1)	0.32 ± 0.05	6.5	40	★

TABLE 5 This table lists the equatorial coordinates (α , δ for epoch 2016.0) of all detected co-moving companions (sorted by their identifier) together with their derived absolute G-band magnitude M_G , projected separation sep , mass, and effective temperature T_{eff} . The flags for all companions, as defined in the text, are listed in the last column of this table.

TOI	α [°]	δ [°]	M_G [mag]	sep [au]	$mass$ [M_\odot]	T_{eff} [K]	Flags
2689 B	52.67980914211	-22.00574100448	8.60 ^{+0.24} _{-0.39}	2293	0.55 ^{+0.05} _{-0.01}	3644 ⁺⁷⁴ ₋₃₀	PRI BPRP
2690 A	52.22564042075	-19.97980931517	3.06 ^{+0.28} _{-0.27}	5675	1.25 ^{+0.15} _{-0.19}	6582 ⁺⁴⁹⁹ ₋₄₂₂	PRI BPRP
2690 C	52.23140217705	-19.97473504235	6.17 ^{+0.02} _{-0.23}	417	0.72 ^{+0.11} _{-0.10}	5091 ⁺⁵⁸⁷ ₋₄₉₁	BPRP
2690 D	52.22544078874	-19.97920279422	7.82 ^{+0.02} _{-0.23}	5445	0.57 ^{+0.18} _{-0.16}	4119 ⁺¹⁰¹¹ ₋₅₉₁	
2713 B	63.14997314217	-12.31677269638	9.38 ^{+0.17} _{-0.10}	803	0.50 ^{+0.01} _{-0.01}	3439 ⁺⁴³ ₋₁₈	BPRP
2774 B	83.99328101402	-7.69070839901	6.38 ^{+0.13} _{-0.13}	4387	0.77 ^{+0.03} _{-0.03}	4663 ⁺⁸⁷ ₋₁₃₀	PRI BPRP
2803 B	93.11824755581	-23.48812274817	4.26 ^{+0.03} _{-0.10}	9656	0.98 ^{+0.10} _{-0.11}	6127 ⁺²⁶⁸ ₋₂₅₅	PRI BPRP
2816 A	118.34827052025	-36.80303124411	3.39 ^{+0.29} _{-0.16}	4802	1.05 ^{+0.19} _{-0.11}	6124 ⁺⁴¹⁰ ₋₄₃₂	PRI BPRP
2892 B	116.21354153938	-59.55033254810	6.97 ^{+0.12} _{-0.08}	1134	0.77 ^{+0.02} _{-0.07}	4144 ⁺¹³³ ₋₁₄₀	PRI BPRP SHC2
2909 B	135.66762775837	-37.01688685089	4.98 ^{+0.16} _{-0.15}	1471	0.89 ^{+0.07} _{-0.08}	5950 ⁺³³⁶ ₋₃₄₁	BPRP
2911 B	129.08112322060	-46.36535231381	8.74 ^{+0.48} _{-0.48}	408	0.46 ^{+0.04} _{-0.01}	3759 ⁺²³⁶ ₋₂₁₇	BPRP
2956 B	154.07230985168	-55.70815920608	10.22 ^{+0.10} _{-0.11}	7006	0.35 ^{+0.01} _{-0.01}	3397 ⁺²¹ ₋₂₀	BPRP inter
3039 B	153.13022050881	-67.26030381008	10.92 ^{+0.12} _{-0.15}	9581	0.26 ^{+0.02} _{-0.01}	3261 ⁺²⁸ ₋₂₁	BPRP inter
3040 B	151.49952902222	-66.89749884226	4.02 ^{+0.09} _{-0.17}	1587	1.04 ^{+0.10} _{-0.12}	6332 ⁺³³⁵ ₋₃₂₁	PRI BPRP
3073 B	46.56549356037	70.21466583708	10.35 ^{+0.01} _{-0.06}	51	0.31 ^{+0.15} _{-0.10}	3393 ⁺³²⁸ ₋₂₇₇	
3097 B	173.07501259364	-47.49670805769	8.28 ^{+0.02} _{-0.35}	576	0.53 ^{+0.20} _{-0.16}	3943 ⁺¹⁰²² ₋₅₀₄	BPRP
3106 B	198.65051016909	-30.72143684476	10.03 ^{+0.04} _{-0.04}	2951	0.37 ^{+0.01} _{-0.01}	3432 ⁺⁵ ₋₆	BPRP inter
3106 C	198.64882903573	-30.72210050023	10.45 ^{+0.04} _{-0.04}	920	0.32 ^{+0.01} _{-0.01}	3352 ⁺⁸ ₋₈	inter
3106 D	198.65085679278	-30.72111745904	11.32 ^{+0.04} _{-0.04}	3579	0.22 ^{+0.01} _{-0.01}	3197 ⁺⁵ ₋₅	inter
3155 B	203.54694265012	-59.58056427971	9.97 ^{+0.20} _{-0.26}	6699	0.40 ^{+0.01} _{-0.15}	3277 ⁺⁵¹ ₋₁₅₀	BPRP
3159 B	200.46403486980	-62.54097288469	7.37 ^{+0.41} _{-0.41}	1803	0.60 ^{+0.05} _{-0.04}	4403 ⁺⁴⁰⁰ ₋₂₃₃	BPRP
3179 B	155.14254447665	-62.65066542031	6.10 ^{+0.02} _{-0.50}	457	0.73 ^{+0.21} _{-0.16}	5078 ⁺⁸⁷⁵ ₋₉₇₁	
3202 B	212.54548867172	-51.45435224644	10.14 ^{+0.12} _{-0.12}	2496	0.44 ^{+0.02} _{-0.03}	3249 ⁺⁴² ₋₅₁	BPRP SHC2
3205 B	218.47574830405	-24.65345918341	10.37 ^{+0.28} _{-0.50}	500	0.31 ^{+0.14} _{-0.11}	3381 ⁺³³⁸ ₋₂₇₅	
3250 B	210.09591253907	-22.34183472940	4.89 ^{+0.45} _{-0.33}	908	0.91 ^{+0.10} _{-0.09}	5748 ⁺⁴²⁸ ₋₃₆₄	PRI BPRP
3252 B	209.18350344891	-35.29244923624	6.33 ^{+0.18} _{-0.35}	3892	0.77 ^{+0.03} _{-0.03}	4802 ⁺¹⁶⁰ ₋₁₂₆	PRI BPRP
3266 B	270.94813182446	-86.30896563367	5.35 ^{+0.03} _{-0.50}	564	0.82 ^{+0.22} _{-0.18}	5513 ⁺⁷⁶⁵ ₋₁₀₂₀	
3277 B	290.85656623835	-54.33008049712	7.36 ^{+0.46} _{-0.46}	621	0.60 ^{+0.05} _{-0.05}	4345 ⁺²⁵¹ ₋₃₇₁	BPRP
3284 B	295.19066454851	-49.41967226418	10.00 ^{+0.15} _{-0.19}	1949	0.37 ^{+0.01} _{-0.02}	3435 ⁺²⁰ ₋₂₅	BPRP inter
3288 B	297.11065076211	-43.01745378499	9.33 ^{+0.32} _{-0.17}	436	0.39 ^{+0.01} _{-0.04}	3711 ⁺¹⁸³ ₋₂₀₆	BPRP
3294 B	279.64123193685	-62.30216351727	5.18 ^{+0.49} _{-0.43}	655	0.84 ^{+0.24} _{-0.19}	5595 ⁺⁷⁵⁷ ₋₉₇₅	
3314 B	279.61040441412	-40.80284923000	9.93 ^{+0.20} _{-0.25}	1214	0.36 ^{+0.14} _{-0.15}	3467 ⁺⁴²³ ₋₃₁₆	
3342 A	266.37031019423	-56.88307732848	3.17 ^{+0.21} _{-0.27}	7548	1.24 ^{+0.14} _{-0.16}	6737 ⁺⁴⁷⁵ ₋₄₁₇	PRI BPRP
3344 B	272.45063094575	-31.89101009750	8.56 ^{+0.02} _{-0.32}	542	0.50 ^{+0.18} _{-0.15}	3833 ⁺⁸³² ₋₄₁₉	BPRP
3353 B	106.64429307975	-75.82468702824	11.28 ^{+0.23} _{-0.32}	8091	0.30 ^{+0.01} _{-0.01}	2969 ⁺⁶ ₋₆	PRI BPRP
3355 B	79.32283332374	-59.06790375910	9.79 ^{+0.02} _{-0.15}	615	0.39 ^{+0.01} _{-0.01}	3457 ⁺²⁰ ₋₃	BPRP inter
3386 B	114.31707212743	-36.27431755178	10.77 ^{+0.13} _{-0.12}	2262	0.28 ^{+0.01} _{-0.02}	3290 ⁺²³ ₋₂₅	BPRP inter
3398 B	143.54204550775	-7.43466051582	12.66 ^{+0.11} _{-0.17}	1002	0.15 ^{+0.01} _{-0.01}	3030 ⁺²⁵ ₋₁₆	BPRP inter
3444 B	241.28746446466	-46.56653151785	10.54 ^{+0.19} _{-0.21}	1558	0.31 ^{+0.03} _{-0.02}	3334 ⁺⁴¹ ₋₃₇	BPRP inter
3450 B	228.03493229226	-53.31341707455	4.03 ^{+0.23} _{-0.23}	227	0.98 ^{+0.01} _{-0.01}	6098 ⁺¹²⁴ ₋₁₃₈	BPRP inter

TABLE 5 continued

TOI	α [°]	δ [°]	M_G [mag]	sep [au]	$mass$ [M_\odot]	T_{eff} [K]	Flags
3490 A	155.19220256086	-78.83037132449	4.50 ^{+0.16} _{-0.22}	2069	0.97 ^{+0.08} _{-0.08}	5898 ⁺²⁹⁴ ₋₂₅₅	PRI BPRP
3491 B	245.27530424327	-59.50924599551	5.76 ^{+0.31} _{-0.29}	8216	0.84 ^{+0.03} _{-0.04}	5104 ⁺¹²¹ ₋₁₈₈	PRI BPRP
3492 B	166.61723550293	-53.72597472023	13.97 ^{+0.24} _{-0.26}	9467	0.11 ^{+0.01} _{-0.01}	2848 ⁺³⁴ ₋₃₂	BPRP inter
3500 B	186.81755444350	-29.83214647849	6.04 ^{+0.14} _{-0.27}	720	0.69 ^{+0.01} _{-0.04}	5327 ⁺¹⁸⁶ ₋₂₉₁	PRI BPRP
3503 A	163.71599435291	-58.57065780251	1.09 ^{+0.17} _{-0.08}	2533	2.04 ^{+0.20} _{-0.17}	9289 ⁺⁶³³ ₋₅₃₉	PRI BPRP
3504 A	300.72967978564	24.43432813004	3.38 ^{+0.38} _{-0.46}	5275	1.15 ^{+0.15} _{-0.17}	6255 ⁺⁴³⁴ ₋₃₇₇	PRI BPRP
3514 B	295.55733246370	32.61396027509	6.39 ^{+0.14} _{-0.27}	735	0.75 ^{+0.05} _{-0.06}	4809 ⁺²⁹⁸ ₋₁₈₄	
3522 B	301.07877627007	34.39800696820	5.86 ^{+0.19} _{-0.19}	1439	0.79 ^{+0.01} _{-0.01}	5144 ⁺²⁰ ₋₁₇₉	PRI BPRP SHC2
3531 B	321.37489008166	55.72320749049	11.30 ^{+0.28} _{-0.20}	1934	0.23 ^{+0.02} _{-0.02}	3199 ⁺³⁰ ₋₃₄	BPRP inter
3533 A	308.56188357176	35.39520207642	3.88 ^{+0.50} _{-0.46}	612	1.04 ^{+0.14} _{-0.12}	6252 ⁺³⁸⁰ ₋₃₃₇	PRI BPRP
3560 B	296.05666264299	40.30133090433	6.47 ^{+0.10} _{-0.14}	9736	0.75 ^{+0.06} _{-0.01}	4684 ⁺⁹⁷ ₋₁₄₅	PRI BPRP
3584 B	314.89532676098	52.39640704381	5.61 ^{+0.03} _{-0.52}	483	0.79 ^{+0.22} _{-0.19}	5364 ⁺⁷⁸⁴ ₋₁₀₆₈	
3584 C	314.89638340826	52.39894598594	8.45 ^{+0.21} _{-0.21}	4610	0.60 ^{+0.01} _{-0.06}	3694 ⁺¹³⁸ ₋₂₀₁	BPRP
3586 B	310.22786035232	50.92736379220	11.10 ^{+0.02} _{-0.18}	6127	0.30 ^{+0.02} _{-0.01}	3046 ⁺⁵⁵ ₋₂₄	BPRP
3607 B	310.70522263346	58.51513806732	6.91 ^{+0.04} _{-0.49}	445	0.65 ^{+0.19} _{-0.17}	4596 ⁺⁹⁶⁵ ₋₈₄₂	
3628 B	12.86088057204	47.65766502045	4.10 ^{+0.14} _{-0.19}	7458	0.94 ^{+0.13} _{-0.08}	6085 ⁺²⁸⁶ ₋₂₄₀	PRI BPRP
3628 C	12.86142759059	47.65764466259	8.11 ^{+0.14} _{-0.19}	7240	0.58 ^{+0.02} _{-0.02}	3881 ⁺⁷² ₋₅₆	inter
3634 B	12.56953489794	27.56870464509	4.03 ^{+0.23} _{-0.23}	182	1.15 ^{+0.04} _{-0.08}	6098 ⁺¹²⁴ ₋₁₃₈	
3636 B	21.06423146521	32.81104514730	10.79 ^{+0.19} _{-0.18}	1322	0.28 ^{+0.02} _{-0.02}	3286 ⁺³⁵ ₋₃₅	BPRP inter
3642 B	45.14837045982	39.93455028157	9.81 ^{+0.17} _{-0.17}	752	0.36 ^{+0.17} _{-0.13}	3494 ⁺⁴⁰⁷ ₋₃₂₀	
3682 B	50.27236394088	25.30273990370	6.72 ^{+0.22} _{-0.38}	8652	0.65 ^{+0.01} _{-0.03}	4741 ⁺¹⁷⁰ ₋₅₄₂	PRI BPRP
3688 B	39.28139400597	54.85247997963	9.69 ^{+0.27} _{-0.28}	1976	0.40 ^{+0.03} _{-0.02}	3468 ⁺⁶⁴ ₋₂₈	BPRP inter
3712 B	89.23862334799	36.36406003677	9.67 ^{+0.03} _{-0.03}	9188	0.45 ^{+0.01} _{-0.01}	3366 ⁺⁷ ₋₉	BPRP
3714 B	69.55326641769	39.45778406803	13.12 ^{+0.15} _{-0.44}	302			BPRP WD
3724 B	80.42532763791	36.27445179215	7.32 ^{+0.14} _{-0.17}	759	0.65 ^{+0.14} _{-0.10}	4312 ⁺⁹⁷¹ ₋₄₂₀	SHC2
3741 B	81.57756446053	47.07372521578	4.70 ^{+0.43} _{-0.39}	816	0.92 ^{+0.08} _{-0.07}	5920 ⁺³⁰⁴ ₋₃₀₅	
3742 A	72.79961580873	50.09792164393	6.49 ^{+0.42} _{-0.27}	617	0.75 ^{+0.05} _{-0.02}	4677 ⁺¹⁶³ ₋₉₇	PRI BPRP
3745 B	65.61614638996	46.53610430219	5.20 ^{+0.38} _{-0.30}	643	0.84 ^{+0.06} _{-0.06}	5747 ⁺²⁸⁷ ₋₂₈₇	PRI BPRP
3758 B	41.32320343219	69.10594381977	9.34 ^{+0.49} _{-0.43}	624	0.43 ^{+0.18} _{-0.17}	3620 ⁺⁶⁹⁴ ₋₃₅₉	
3761 A	48.67072130313	66.92212577884	5.33 ^{+0.09} _{-0.11}	1087	0.88 ^{+0.04} _{-0.06}	5445 ⁺²⁶¹ ₋₂₃₆	PRI BPRP
3781 B	110.88135381827	50.34642062369	8.06 ^{+0.10} _{-0.53}	3446	0.60 ^{+0.01} _{-0.01}	3888 ⁺¹⁴² ₋₆₃	PRI BPRP
3791 B	295.38708444765	56.21513543548	3.92 ^{+0.17} _{-0.09}	4692	1.07 ^{+0.12} _{-0.12}	6262 ⁺³⁷⁸ ₋₃₃₇	PRI BPRP
3795 B	98.73110756335	49.67435429421	8.27 ^{+0.04} _{-0.16}	3736	0.55 ^{+0.01} _{-0.01}	3877 ⁺¹⁷ ₋₁₇	PRI BPRP
3797 B	104.84307868700	48.30487763435	6.58 ^{+0.15} _{-0.38}	3563	0.75 ^{+0.05} _{-0.02}	4640 ⁺¹²² ₋₉₅	PRI BPRP
3801 B	114.01080278850	47.25894442431	9.57 ^{+0.30} _{-0.14}	1459	0.41 ^{+0.01} _{-0.03}	3494 ⁺³³ ₋₄₅	BPRP inter
3823 B	127.03203872903	56.43099174198	9.64 ^{+0.16} _{-0.14}	1490	0.40 ^{+0.01} _{-0.01}	3477 ⁺³³ ₋₂₁	BPRP inter
3828 B	150.89193313396	67.99037362147	3.40 ^{+0.25} _{-0.25}	501	1.29 ^{+0.07} _{-0.08}	6457 ⁺¹⁷⁶ ₋₁₇₀	BPRP inter
3829 B	137.42163520494	31.29264394692	6.07 ^{+0.29} _{-0.23}	578	0.79 ^{+0.02} _{-0.04}	4925 ⁺¹⁶⁸ ₋₂₀₆	BPRP inter
3867 B	193.65507319999	47.06549457455	10.09 ^{+0.25} _{-0.13}	1318	0.37 ^{+0.01} _{-0.03}	3422 ⁺¹⁷ ₋₄₉	BPRP inter
3872 B	162.38755782729	27.19025918622	5.80 ^{+0.21} _{-0.32}	938	0.74 ^{+0.05} _{-0.05}	5392 ⁺³⁴⁸ ₋₃₃₁	PRI BPRP
3875 B	204.08561299815	68.52200415724	5.38 ^{+0.46} _{-0.30}	7220	0.87 ^{+0.05} _{-0.03}	5228 ⁺³³⁷ ₋₁₁₀	PRI BPRP NSS
3883 B	183.96410252047	47.42821260192	8.40 ^{+0.41} _{-0.30}	2601	0.64 ^{+0.01} _{-0.01}	3817 ⁺²⁴ ₋₂₃	BPRP
3889 B	180.25780661146	55.84614755703	6.80 ^{+0.50} _{-0.53}	698	0.70 ^{+0.04} _{-0.01}	4586 ⁺¹²⁵ ₋₁₀₅	PRI BPRP

TABLE 5 continued

TOI	α [°]	δ [°]	M_G [mag]	sep [au]	$mass$ [M_\odot]	T_{eff} [K]	Flags
3896 B	187.93969685290	63.90585576769	9.41 ^{+0.14} _{-0.19}	3274	0.45 ^{+0.01} _{-0.01}	3480 ⁺²² ₋₆₁	PRI BPRP
3915 B	205.48821304826	17.30005590348	10.97 ^{+0.03} _{-0.05}	476	0.25 ^{+0.14} _{-0.10}	3268 ⁺³¹⁶ ₋₂₈₂	
3920 B	336.69063547736	57.43370262278	7.71 ^{+0.32} _{-0.25}	841	0.58 ^{+0.18} _{-0.17}	4162 ⁺¹⁰⁰⁹ ₋₆₁₆	
3922 A	228.83275054542	40.26678851965	4.80 ^{+0.10} _{-0.10}	550	0.90 ^{+0.06} _{-0.07}	5904 ⁺²⁹⁵ ₋₂₉₆	PRI BPRP
3956 A	229.21827948120	51.39777270307	3.93 ^{+0.15} _{-0.25}	1760	0.98 ^{+0.12} _{-0.09}	5979 ⁺³⁶¹ ₋₂₈₀	PRI BPRP NSS
3966 B	225.38169817837	38.53370077153	10.10 ^{+0.17} _{-0.23}	828	0.36 ^{+0.02} _{-0.02}	3420 ⁺²⁹ ₋₃₃	BPRP inter
3977 B	231.12743053572	46.69506834347	5.65 ^{+0.18} _{-0.38}	659	0.74 ^{+0.04} _{-0.04}	5616 ⁺²⁵⁵ ₋₃₂₂	PRI BPRP
3984 B	226.33680816581	36.78784975544	13.68 ^{+0.16} _{-0.16}	356			BPRP WD
3998 B	7.63787900943	56.33181795423	9.38 ^{+0.02} _{-0.23}	885	0.42 ^{+0.17} _{-0.15}	3606 ⁺⁵⁴² ₋₃₄₃	BPRP
4001 B	2.52363216857	64.57429750735	6.18 ^{+0.04} _{-0.19}	3245	0.77 ^{+0.03} _{-0.04}	4891 ⁺²⁰⁰ ₋₁₃₂	PRI BPRP
4021 B	28.65074517816	64.56885859645	5.98 ^{+0.29} _{-0.25}	5639	0.79 ^{+0.02} _{-0.05}	5071 ⁺⁵⁸⁴ ₋₂₂₈	PRI BPRP
4040 B	268.61512748281	77.48923373608	13.01 ^{+0.07} _{-0.15}	989	0.14 ^{+0.01} _{-0.01}	2979 ⁺²² ₋₁₀	BPRP inter
4059 B	274.18010202664	76.89014057693	8.25 ^{+0.11} _{-0.19}	1199	0.45 ^{+0.01} _{-0.01}	4265 ⁺²¹⁹ ₋₄₃₉	BPRP
4070 A	250.27677877596	42.43723126784	3.95 ^{+0.07} _{-0.19}	1532	0.99 ^{+0.13} _{-0.10}	6316 ⁺³⁶² ₋₃₀₅	PRI BPRP
4077 B	250.30191634926	38.96497231403	10.53 ^{+0.11} _{-0.20}	4731	0.35 ^{+0.01} _{-0.01}	3256 ⁺⁴ ₋₃	BPRP SHC2
4079 A	19.97560713621	64.53580319915	3.51 ^{+0.18} _{-0.18}	4168	1.20 ^{+0.09} _{-0.14}	6660 ⁺⁴³⁶ ₋₃₈₂	PRI BPRP
4081 B	21.57135203059	64.83988013998	5.17 ^{+0.35} _{-0.35}	980	0.93 ^{+0.05} _{-0.05}	5450 ⁺²⁰⁰ ₋₁₆₃	BPRP inter
4089 B	267.85149807828	22.66149859234	5.84 ^{+0.02} _{-0.51}	426	0.77 ^{+0.21} _{-0.18}	5237 ⁺⁸³⁴ ₋₁₀₅₈	
4107 B	269.24657644488	58.88101313795	8.78 ^{+0.13} _{-0.35}	1898	0.55 ^{+0.01} _{-0.01}	3584 ⁺⁵¹ ₋₃₁	BPRP
4113 B	283.89266583485	71.40095184180	11.54 ^{+0.02} _{-0.27}	531	0.21 ^{+0.01} _{-0.01}	3170 ⁺³³ ₋₃	BPRP inter
4123 B	131.23352602350	75.10638543419	10.90 ^{+0.07} _{-0.08}	620	0.27 ^{+0.01} _{-0.01}	3265 ⁺¹⁵ ₋₁₂	BPRP inter
4128 B	128.23671176505	82.03039044190	6.08 ^{+0.19} _{-0.21}	7354	0.79 ^{+0.06} _{-0.04}	4946 ⁺¹⁹¹ ₋₁₇₇	PRI BPRP NSS
4145 B	39.43164905049	80.26774459975	11.34 ^{+0.09} _{-0.17}	356	0.21 ^{+0.14} _{-0.07}	3173 ⁺³⁰² ₋₂₈₉	
4168 B	173.82185450357	79.41401164812	6.91 ^{+0.13} _{-0.22}	2804	0.70 ^{+0.04} _{-0.01}	4443 ⁺¹⁴⁴ ₋₁₂₁	PRI BPRP
4175 B	198.53969402570	-16.55942836813	4.58 ^{+0.21} _{-0.21}	75	0.95 ^{+0.09} _{-0.09}	6082 ⁺²⁹⁴ ₋₂₆₈	BPRP
4175 C	198.54163019207	-16.60566374031	10.44 ^{+0.05} _{-0.29}	7727	0.35 ^{+0.01} _{-0.01}	3240 ⁺¹⁵ ₋₄₄	PRI BPRP
4176 B	201.99815807515	-29.78494557416	5.82 ^{+0.03} _{-0.19}	9366	0.74 ^{+0.03} _{-0.04}	5351 ⁺¹⁶⁶ ₋₁₆₈	PRI BPRP
4179 A	202.41900469667	-16.56534510191	4.74 ^{+0.08} _{-0.21}	3615	0.94 ^{+0.06} _{-0.09}	5882 ⁺²⁴⁸ ₋₂₄₂	PRI BPRP
4182 B	45.90781719137	-69.74348706667	10.93 ^{+0.02} _{-0.19}	2315	0.25 ^{+0.01} _{-0.01}	3278 ⁺¹¹ ₋₆₁	PRI BPRP
4192 B	23.78717048262	-41.50697537823	5.49 ^{+0.13} _{-0.12}	1332	0.75 ^{+0.05} _{-0.04}	5702 ⁺²⁷⁵ ₋₃₂₆	PRI BPRP
4212 B	116.38141838603	-25.99214271609	12.72 ^{+0.32} _{-0.32}	7221	0.15 ^{+0.01} _{-0.01}	3021 ⁺⁴⁵ ₋₄₆	
4226 B	116.96489620573	-25.56643169835	11.08 ^{+0.44} _{-0.46}	2226	0.25 ^{+0.06} _{-0.03}	3233 ⁺⁸⁶ ₋₆₀	BPRP inter
4245 B	125.80648008533	-45.79287939591	10.65 ^{+0.16} _{-0.30}	346	0.30 ^{+0.14} _{-0.11}	3325 ⁺³¹³ ₋₂₆₈	
4293 B	302.97797038614	-49.00095806061	9.40 ^{+0.11} _{-0.18}	1170	0.43 ^{+0.02} _{-0.01}	3534 ⁺⁴⁰ ₋₂₆	BPRP inter
4301 B	166.26442627031	-46.03699476689	13.21 ^{+0.08} _{-0.10}	4984			WD
4303 B	72.35767076023	-43.35604073937	7.86 ^{+0.18} _{-0.32}	2309	0.60 ^{+0.01} _{-0.01}	3992 ⁺¹²¹ ₋₇₃	PRI BPRP
4325 B	101.84813744489	6.13570650776	11.87 ^{+0.26} _{-0.20}	1296	0.22 ^{+0.01} _{-0.01}	2972 ⁺⁸ ₋₅₁	PRI BPRP
4330 B	220.35023214342	-33.94988039998	4.25 ^{+0.02} _{-0.29}	628	0.96 ^{+0.29} _{-0.16}	5943 ⁺⁷⁷⁹ ₋₅₅₉	
4337 A	164.28776576746	-69.98061944588	4.89 ^{+0.06} _{-0.18}	332	0.94 ^{+0.06} _{-0.06}	5619 ⁺²³⁶ ₋₂₁₁	PRI BPRP
4339 A	212.92908519599	-29.97493629373	8.51 ^{+0.16} _{-0.36}	448	0.55 ^{+0.01} _{-0.01}	3728 ⁺³⁰ ₋₂₇	PRI BPRP
4344 B	69.64989596367	-61.34368885093	9.32 ^{+0.01} _{-0.17}	486	0.42 ^{+0.18} _{-0.15}	3627 ⁺⁶¹⁸ ₋₃₅₄	
4349 B	0.12979485849	-26.23033985535	10.25 ^{+0.27} _{-0.30}	193	0.30 ^{+0.01} _{-0.05}	3475 ⁺⁶⁵ ₋₁₉₁	BPRP

TABLE 5 continued

TOI	α [°]	δ [°]	M_G [mag]	sep [au]	$mass$ [M_\odot]	T_{eff} [K]	Flags
4350 B	32.88391134546	-76.10637329379	9.52 ^{+0.11} _{-0.17}	393	0.41 ^{+0.05} _{-0.02}	3489 ⁺¹³⁹ ₋₁₂₈	BPRP
4359 B	149.73699892763	-53.30425173334	9.37 ^{+0.14} _{-0.16}	2728	0.45 ^{+0.01} _{-0.01}	3497 ⁺⁶⁴ ₋₆₄	PRI BPRP
4366 B	180.29004388300	-67.75581738345	7.53 ^{+0.46} _{-0.38}	4870	0.60 ^{+0.01} _{-0.01}	4133 ⁺¹³⁵ ₋₆₅	PRI BPRP
4369 B	100.58750610095	-58.18153364282	2.94 ^{+0.17} _{-0.17}	1736	1.31 ^{+0.12} _{-0.22}	6369 ⁺⁴²⁰ ₋₄₆₉	PRI BPRP
4370 B	201.46970099045	-16.42600768553	9.90 ^{+0.03} _{-0.05}	6604	0.40 ^{+0.01} _{-0.01}	3381 ⁺⁷⁴ ₋₅₅	PRI BPRP
4372 B	218.85166922760	-76.21442871924	12.32 ^{+0.14} _{-0.26}	629	0.17 ^{+0.01} _{-0.01}	3076 ⁺³² ₋₁₇	BPRP inter
4390 B	262.64794769062	-52.33654991895	3.36 ^{+0.18} _{-0.18}	212	1.30 ^{+0.05} _{-0.05}	6483 ⁺¹²⁷ ₋₁₂₀	BPRP inter
4414 A	267.47501105883	-37.53114551499	2.25 ^{+0.04} _{-0.04}	291	1.80 ^{+0.02} _{-0.01}	7633 ⁺⁸⁵ ₋₈₁	inter
4420 B	246.80051205533	-69.34279402648	6.07 ^{+0.18} _{-0.15}	1062	0.85 ^{+0.01} _{-0.01}	4898 ⁺¹⁵⁹ ₋₂₉	PRI BPRP SHC2 NSS
4425 B	264.84072608556	-35.39308157571	8.84 ^{+0.21} _{-0.24}	879	0.49 ^{+0.01} _{-0.01}	3732 ⁺²⁹ ₋₂₃	BPRP SHC2
4463 B	279.36130629852	18.72900308391	10.14 ^{+0.20} _{-0.21}	2009	0.40 ^{+0.01} _{-0.01}	3271 ⁺¹⁰ ₋₉	PRI BPRP
4499 B	284.36118628028	39.07217949918	11.35 ^{+0.08} _{-0.10}	2566	0.27 ^{+0.01} _{-0.01}	3023 ⁺⁸ ₋₆	BPRP
4522 B	23.30225457564	5.64522664713	11.30 ^{+0.11} _{-0.11}	1589	0.23 ^{+0.01} _{-0.01}	3199 ⁺¹⁴ ₋₁₃	BPRP inter
4546 A	51.43958735455	23.18677535559	2.03 ^{+0.27} _{-0.27}	2478	1.61 ^{+0.22} _{-0.17}	7354 ⁺⁷⁰³ ₋₅₈₇	PRI BPRP

TABLE 5 continued

CTOI	α [°]	δ [°]	M_G [mag]	sep [au]	$mass$ [M_\odot]	T_{eff} [K]	Flags
13073396 B	348.05671579910	-27.36857356304	12.25 ^{+0.08} _{-0.07}	4961			BPRP WD
37652870 B	2.18607214877	-7.85952561311	11.30 ^{+0.22} _{-0.15}	5393	0.25 ^{+0.01} _{-0.01}	3110 ⁺⁵⁴ ₋₈	PRI BPRP
94984950 B	250.46683181731	-32.80896712763	12.46 ^{+0.23} _{-0.21}	2212	0.16 ^{+0.01} _{-0.01}	3059 ⁺²⁶ ₋₃₃	BPRP inter
145601161 B	132.53210895700	-50.58986267488	9.36 ^{+0.35} _{-0.37}	2885	0.30 ^{+0.07} _{-0.01}	3404 ⁺⁵⁰ ₋₆₆	PRI BPRP
219018744 B	224.05793485662	65.90175921968	5.61 ^{+0.34} _{-0.35}	4889	0.83 ^{+0.03} _{-0.05}	5267 ⁺¹⁸⁴ ₋₁₄₀	PRI BPRP
228463329 B	357.88303738396	-17.87044137990	11.04 ^{+0.09} _{-0.38}	1157	0.30 ^{+0.01} _{-0.01}	3075 ⁺¹⁰⁷ ₋₄₇	PRI BPRP
248960573 B	22.04582289281	-5.85324705803	6.14 ^{+0.02} _{-0.02}	174	0.79 ^{+0.01} _{-0.01}	4874 ⁺¹⁵ ₋₁₅	BPRP inter
323717669 B	348.05522686404	59.48812294573	10.03 ^{+0.05} _{-0.07}	550	0.35 ^{+0.15} _{-0.13}	3434 ⁺³⁷⁹ ₋₂₉₁	
333785427 B	307.77636541596	75.81199093489	6.13 ^{+0.02} _{-0.50}	551	0.73 ^{+0.20} _{-0.17}	5066 ⁺⁸⁷⁹ ₋₉₉₀	
345327044 B	355.70113206370	59.18699040797	10.25 ^{+0.15} _{-0.08}	5621	0.35 ^{+0.04} _{-0.01}	3304 ⁺⁷ ₋₄₂	PRI BPRP